PART I

Measures and Identifications

Chapter 1

Identification of Induction Motor in Sinusoidal Mode

1.1. Introduction

Models generally used in electrical engineering are obtained from the laws of physics and are based on the knowledge of a certain number of parameters, they are called parametric models. As with the model structure, knowledge of parameters can also be obtained from laws of physics, if modeling is pushed far enough. Nevertheless, this approach has a few drawbacks: calculations are often fastidious; parameters depend on geometry and the materials used, which may not be well known. In addition, some parameters may vary during the life of a system and this is difficult to model by applying the laws of physics.

Another approach, that is more pragmatic, consists of estimating the numeric values of parameters so that the model has the same behavior as the experimental system. In this chapter, we will focus on the estimation procedures for the induction machine parameters from sinusoidal mode measurements. The methods we will present apply to all types of induction machines and are not based on usual stator measurements and rotation speed. First, we will develop the parametric models liable to use this type of estimation procedure. We will then present the most basic methods based on a limited number of measurements. In order to improve estimation precision, it may be necessary to use a larger number of measurements. We will present two methods with this possibility.

Chapter written by Edouard LAROCHE and Jean-Paul LOUIS.

Electrical Actuators: Identification and Observation Edited by Bernard de Fornel and Jean-Paul Louis

1.2. The models

The sinusoidal mode is not a steady-state mode strictly speaking because the electrical variables are not constant. In order to obtain the model rigorously, it is necessary to rely on the actuator's dynamic model.

1.2.1. *Dynamic model of the induction machine*

For the establishment of the dynamic model, consider a wound rotor three-phase induction machine. We presume that the stator and rotor windings are perfectly symmetrical (hypothesis of concentricity). We use the hypothesis of the first space harmonic, i.e. we presume that magnetomotive forces created by windings are sinusoidal space functions. We ignore salience effects and teeth harmonics. Subsequently, we will presume that the model is valid for squirrel-cage machines, a more widespread technology.

First, take the dynamic model of the three-phase induction machine which, for the purpose of this report, is presumed to be star connected. We can detect the three phases by indices a, b, and c. We write i for currents, v voltage, and ϕ fluxes. The resistance of the stator winding is R_s, and the rotor circuit is R_r. We note L_s as the cyclic inductance of the stator, L_r for the rotor, and M is the cyclic mutual inductance between stator and rotor. The machine has p pole pairs.

A set of balanced three-phase stator quantities $\{x_{sa}(t),\ x_{sb}(t),\ x_{sc}(t)\}$ without homopolar can be represented by the complex phasor referred to the stator [LOU 04]:

$$\underline{x}_s(t) = \sqrt{\frac{2}{3}}\ \left(x_{sa}(t) + a\, x_{sb}(t) + a^2\, x_{sc}(t)\right) \qquad [1.1]$$

with $a = \exp(j\,\frac{2\pi}{3})$, corresponding to the first component of the Fortescue transform. This transformation is inversible with

$$\begin{bmatrix} x_{sa}(t) \\ x_{sb}(t) \\ x_{sc}(t) \end{bmatrix} = \sqrt{\frac{2}{3}} \begin{bmatrix} \mathrm{Re}(\underline{x}_s(t)) \\ \mathrm{Re}(a\,\underline{x}_s(t)) \\ \mathrm{Re}(a^2\,\underline{x}_s(t)) \end{bmatrix} \qquad [1.2]$$

For a three-phase rotor quantity $\{x_{ra}(t),\ x_{rb}(t),\ x_{rc}(t)\}$, we define the complex phasor referred to the stator, corresponding to the first component of the Ku transform:

$$\underline{x}_r(t) = \sqrt{\frac{2}{3}}\ \exp(j\,p\,\theta(t)) \cdot \left(x_{ra}(t) + a\, x_{rb}(t) + a^2\, x_{rc}(t)\right) \qquad [1.3]$$

where $\theta(t)$ is the angular position of the rotor.

The resulting model is expressed in two series of equations, equations to fluxes

$$\begin{cases} \underline{\phi}_s(t) &= L_s\, \underline{i}_s(t) + M\, \underline{i}_r(t) \\ \underline{\phi}_r(t) &= M\, \underline{i}_s(t) + L_r\, \underline{i}_r(t) \end{cases} \quad [1.4]$$

and voltage equations

$$\begin{cases} \underline{v}_s(t) &= R_s\, \underline{i}_s(t) + \dfrac{d\underline{\phi}_s(t)}{dt} \\ 0 &= R_r\, \underline{i}_r(t) + \dfrac{d\underline{\phi}_r(t)}{dt} - j\, p\, \Omega(t)\, \underline{\phi}_r(t) \end{cases} \quad [1.5]$$

In the second equation, a zero voltage appears in the rotor corresponding to winding short circuit, and an electromotive force proportional to rotation speed Ω of the rotor, resulting from the change in reference frame of rotor variables.

This model depends on five parameters: two resistances R_s and R_r and three inductances: L_s, L_r, and M. The goal of an estimation procedure is to determine the numeric values of these parameters. And yet, this model cannot directly be used. In fact, an infinite number of parameter values correspond to an identical stator behavior [POL 67]. We say that this model is unidentifiable.

1.2.2. *Establishment of the four parameter models*

1.2.2.1. *Total rotor leakage model*

These equations are similar to those of a transformer. As with this other electromagnetic system, we can introduce the magnetizing current relative to stator flux:

$$\underline{\phi}_s = L_s\, \underline{i}_{m\,s} \quad [1.6]$$

implying that

$$\underline{i}_{m\,s} = \underline{i}_s + \frac{M}{L_s}\, \underline{i}_r \quad [1.7]$$

By noting $m_s = \frac{M}{L_s}$ the stator/rotor transformation ratio and $\underline{i}_{2s} = m_s \, \underline{i}_r$ the rotor current referred to the stator, we can write the rotor flux in the following form:

$$\underline{\phi}_r = M \, \underline{i}_{m\,s} + \left(\frac{L_s \, L_r}{M} - M \right) \underline{i}_{2s} \qquad [1.8]$$

We define the total rotor leakage inductance referred to the stator:

$$N_r = \frac{\sigma L_r}{{m_s}^2} \qquad [1.9]$$

where $\sigma = (1 - \frac{M^2}{L_s \, L_r})$ is the *dispersion coefficient*, representative of the leakage part in the magnetic flux. The rotor flux referred to the stator is

$$\underline{\phi}_{2s} = L_s \, \underline{i}_{m\,s} + N_r \, \underline{i}_{2s} \qquad [1.10]$$

and the rotor resistance referred to the stator is $R_{2s} = \frac{R_r}{{m_s}^2}$. The model, referred to as the stator, is in the following form:

$$\begin{cases} \underline{v}_s(t) \;=\; R_s \, \underline{i}_s(t) + \dfrac{d\underline{\phi}_s(t)}{dt} \\ \\ 0 \;=\; R_{2s} \, \underline{i}_{2s}(t) + \dfrac{d\underline{\phi}_{2s}(t)}{dt} - j \, p \, \Omega(t) \, \underline{\phi}_{2s}(t) \end{cases} \qquad [1.11]$$

The model is then described by equations [1.6], [1.10], and [1.11] and is given in Figure 1.1. There are four parameters (R_s, R_{2s}, L_s, and N_r), illustrated in Table 1.1, instead of five and are identifiable. Once these four parameters are identified, the parameters of the initial model are obtained in the following way: since L_s and R_s are already known, R_r, M, and L_r must still be determined with the help of two equations. The system is therefore underdetermined, and we must impose a parameter. We will arbitrarily choose the value of m_s. We then get $R_r = {m_s}^2 \, R_{2s}$, $M = m_s \, L_s$, and $L_r = {m_s}^2 \, (L_s + N_r)$.

1.2.2.2. *Total stator leakage model*

Another possibility of writing a model based on four parameters is to define the magnetizing current from the rotor flux:

$$\underline{\phi}_r = M \, \underline{i}_{m\,r} \qquad [1.12]$$

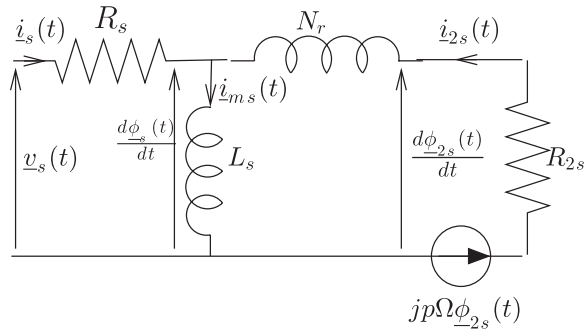

Figure 1.1. *Dynamic total rotor leakage model referred to the stator*

Generic parameter	Rotor leakage	Stator leakage
m	$m_s = \frac{M}{L_s}$	$m_r = \frac{L_r}{M}$
R_s	R_s	R_s
N	$N_r = \frac{\sigma L_r}{{m_s}^2}$	$N_s = \sigma L_s$
L_m	$L_{ms} = L_s$	$L_{mr} = \frac{M^2}{L_r} = (1-\sigma) L_s$
R_2	$R_{2s} = \frac{R_r}{{m_s}^2}$	$R_{2r} = \frac{R_r}{{m_r}^2}$

Table 1.1. *Parameters of the four-parameter dynamic models*

Resulting in node law $\underline{i}_s + m_r\,\underline{i}_r = \underline{i}_{mr}$ with $m_r = \frac{L_r}{M}$. By defining the inductance of total leakages referred to the stator:

$$N_s = \sigma\, L_s \qquad [1.13]$$

and the magnetizing inductance $L_{mr} = \frac{M^2}{L_r}$, the stator flux is written as

$$\underline{\phi}_s = N_s\,\underline{i}_s + L_{mr}\,\underline{i}_{mr}. \qquad [1.14]$$

By noting the variables referred to the stator $\underline{i}_{2r} = m_r\,\underline{i}_r$, $R_{2r} = \frac{R_r}{{m_r}^2}$, and $\underline{\phi}_{2r} = \underline{\phi}_r/m_r$, we rewrite the following flux equations:

$$\left\{\begin{array}{rcl} \underline{\phi}_s(t) & = & N_s\,\underline{i}_s(t) + L_{mr}\,\underline{i}_{mr}(t) \\ \underline{\phi}_{2r}(t) & = & L_{mr}\,\underline{i}_{mr}(t) \end{array}\right. \qquad [1.15]$$

and voltage equations

$$\begin{cases} \underline{v}_s(t) \;=\; R_s\, \underline{i}_s(t) + \dfrac{d\underline{\phi}_s(t)}{dt} \\ \\ 0 \;=\; R_{2r}\, \underline{i}_{2r}(t) + \dfrac{d\underline{\phi}_{2r}(t)}{dt} - j\, p\, \Omega(t)\, \underline{\phi}_{2r}(t) \end{cases} \qquad [1.16]$$

The model defined by equations [1.15] and [1.16] is presented in Figure 1.2. It depends on four parameters (R_s, R_{2r}, N_s, and L_{mr}), illustrated in Table 1.1. Suppose that these parameters are estimated, the parameters of the initial model are then obtained by arbitrarily setting the m_r transformation ratio:

$$\begin{cases} R_r \;=\; {m_r}^2\, R_{2r} \\ L_s \;=\; L_{mr} + N_s \\ M \;=\; m_r\, L_{mr} \\ L_r \;=\; {m_r}^2\, L_{mr} \end{cases} \qquad [1.17]$$

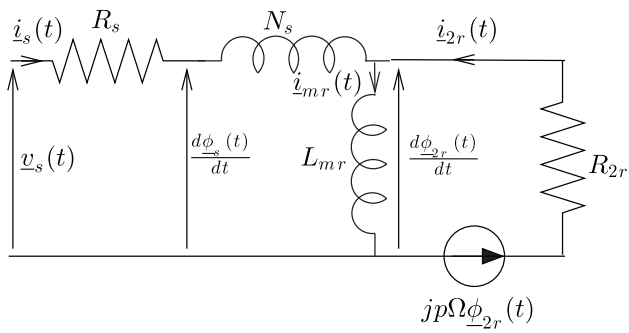

Figure 1.2. *Dynamic total stator leakage model referred to the stator*

1.2.2.3. *Equivalence of total leakage models*

Since the total rotor or stator leakage models are equivalent to the initial model, they are therefore equivalent between each other, and we can go from one to the other by

$$\begin{cases} L_s \;=\; L_{mr} + N_s \\ R_{2s} \;=\; \left(\frac{L_{mr}+N_s}{L_{mr}}\right)^2 R_{2r} \\ N_r \;=\; \left(\frac{L_{mr}+N_s}{L_{mr}}\right) N_s \end{cases} \qquad [1.18]$$

The inverse of these relations results in

$$\begin{cases} L_{mr} &= \dfrac{{L_s}^2}{L_s + N_r} \\ R_{2r} &= \left(\dfrac{L_s}{L_s + N_r}\right)^2 R_{2s} \\ N_s &= \left(\dfrac{L_s}{L_s + N_r}\right) N_r \end{cases} \qquad [1.19]$$

These different equations reveal a single factor, which is less than 1:

$$\frac{m_s}{m_r} = 1 - \sigma = \frac{L_{mr}}{L_{mr} + N_s} = \frac{L_s}{L_s + N_r} \qquad [1.20]$$

1.2.3. *Magnetic circuit saturation*

The increase in the magnetic field in certain parts of the machine's magnetic circuit leads to an decrease in their permeability, creating a magnetic saturation phenomenon. We generally consider that this phenomenon only affects the mutual stator/rotor flux. In fact, leakage fluxes go through a large portion of air and because of that they are less sensitive to the saturation of magnetic parts. We now separate the fluxes in a main flux, noted ϕ_m and leakage fluxes:

$$\begin{cases} \underline{\phi}_s(t) &= l_s\, \underline{i}_s(t) + \underline{\phi}_m(t) \\ \underline{\phi}_r(t) &= l_r\, \underline{i}_r(t) + m\, \underline{\phi}_m(t) \end{cases} \qquad [1.21]$$

where m is the transformation ratio, equal to the number of turn ratio, and l_s and l_r are the leakage inductances of the stator and rotor, respectively, presumed to be constant. We also define the magnetizing current relative to the air-gap flux:

$$\underline{i}_m = \underline{i}_s + m\, \underline{i}_r. \qquad [1.22]$$

By presuming that the saturation acts as a non-uniform fictitious increase of the air-gap and limiting to a development in the first order of this air-gap, it has been shown that the equations of the induction machine remain valid as long as we consider a variable magnetizing inductance L_m, defined by $\underline{\phi}_m = L_m\, \underline{i}_m$, depending on the level of saturation [LEM 99]. We can then choose as a variable, representative of the state

of saturation, the amplitude of the magnetic flux and we note $L_m = L_m(\phi_m)$, or the amplitude of the magnetizing current and we note $L_m = L_m(i_m)$. In what follows, we will note ξ_m the saturation variable that can be equal to i_m or to ϕ_m.

In the absence of the rotor measurement, the transformation ratio is not available and can anyway be arbitrarily chosen with no effect on the behavior of the model referred to the stator. The model then depends on four constant parameters (R_s, R_r, l_s, and l_r) and a characteristic $L_m(.)$.

Saturation can be taken into consideration in two ways in the model: by noting the different values of L_m based on the saturation variable in a table, or by attempting to interpolate this characteristic by a parametered function. In the last case, it is practical to determine the magnetizing current according to flux ($i_m(\phi_m)$), which can be easily done from a polynomial development of the form:

$$i_m = \sum_{k=1}^{n} a_k \, {\phi_m}^k, \qquad [1.23]$$

which is also written $\phi_m = L_m(\phi_m)\, i_m$ with

$$L_m(\phi_m) = \frac{1}{\sum_{k=1}^{n} a_k \, {\phi_m}^{k-1}} \qquad [1.24]$$

Other authors prefer to use a development of L_m according to magnetizing current i_m. We can then use the same form of development. In any case, this consists in choosing a characteristic in the form:

$$L_m(\xi_m) = \frac{L_{m0}}{1 + \sum_{k=1}^{n-1} \alpha_k \, {\xi_m}^k} \qquad [1.25]$$

where $L_{m0} = \frac{1}{a_1}$ is the no-load inductance and $\alpha_k = \frac{a_{k+1}}{a_1}$. In practice, we choose a reduced number of non-zero factors α_k, in order to limit the number of parameters to estimate.

When we consider saturation, leakage separation between stator and rotor is theoretically possible because of saturation. In practice, it is difficult to determine experimentally because the measurement errors produce estimation errors of high order[1]. We can then decide to work on similar models with total leakage at the stator or the rotor. The advantage of working with a model with better identifiability largely compensates slight loss in precision.

1 This result will be demonstrated in the following sections.

1.2.4. *Iron losses*

Field variations in the magnetic circuit of the machine lead to ferromagnetic losses. A first source of magnetic loss is caused by eddy currents, which are currents induced by field variations (also known as Foucault currents). Their power is proportional to the square of the field amplitude and the square of the frequency. The solution to decrease them is to use foliated material circuits.

Hysteresis losses are a second type of magnetic loss. They are connected to the depth of the hysteresis cycle of the magnetic material characteristic. Their power is proportional to the frequency and function of the surface of the cycle run. This surface increases in a non-linear way according to the field amplitude. Different approximations can be proposed to parameter this surface based on the field amplitude. One of them proposes that this surface is proportional to the square of the field amplitude. In any case, these losses can only be calculated for one period.

Eddy current losses are well modeled by a resistance added to the model in parallel to magnetizing inductance. For hysteresis losses, we generally use the same model, which has the advantage of making modeling of all magnetic losses by a single resistance possible. Nevertheless, in this last case, it is an approximation. To be more precise in writing the model, we could parameter the value of the resistance according to frequency, and possibly to the magnetic field amplitude. Nevertheless, in this chapter, we will only consider the case where iron losses are modeled by a single additional resistance, only adding one parameter to models previously presented.

Based on what we have just written, the resistance must be parallel to the magnetizing inductance, which corresponds to the main flux. If we ignore saturation, we then have a model with six parameters (resistances R_s and R_r, leakage inductances l_s and l_r, magnetization inductance L_m, and resistance of iron losses R_f). This model, as we will see later, can theoretically be identified when R_f is not infinite. However, as in the saturation case, leaks are difficult to separate because of the high sensitivity with respect to measurement errors. We then use in practice five parameter models with a single leakage inductance.

1.2.5. *Sinusoidal mode*

In sinusoidal mode (SM), each three-phase system $\{x_a(t),\ x_b(t),\ x_c(t)\}$ can be written in the following form:

$$\begin{cases} x_a(t) &= X\sqrt{2}\cos(\omega t + \alpha_x) \\ x_b(t) &= X\sqrt{2}\cos(\omega t + \alpha_x - \dfrac{2\pi}{3}) \\ x_c(t) &= X\sqrt{2}\cos(\omega t + \alpha_x + \dfrac{2\pi}{3}) \end{cases} \qquad [1.26]$$

In a balanced mode, we can restrict to studying the first phase that is characterized by complex amplitude $\underline{X} = X \exp(j\,\alpha_x)$ (equivalent to the Fresnel vector). The Fortescue component, obtained according to [1.1], is written as

$$\underline{x}(t) = \sqrt{3}\,X\,\exp(j\,(\omega\,t + \alpha_x)) \qquad [1.27]$$

Except for factor $\sqrt{3}\,\exp(j\omega t)$, both notations are equivalent. In this way, all the models developed so far are equally valid for representing the equivalent diagram of the machine. We just have to replace the complex phasors noting the voltage, currents, and flux by the complex amplitudes by noting these same quantities for a phase of the machine.

By noting g as the slip, the rotor rotation speed is linked to the stator angular frequency by the $p\,\Omega = \omega\,(1-g)$ relation. We will again use the equation of the rotor voltage [1.5.b]. It is now written as $0 = R_r\,\underline{I}_r + j\,\omega\,\underline{\Phi}_r - j\,p\,\Omega\,\underline{\Phi}_r$, where $\underline{I}_r$ is the complex amplitude of the current of a rotor phase, written again by dividing by g:

$$j\,\omega\,\underline{\Phi}_r = -\frac{R_r}{g}\,\underline{I}_r \qquad [1.28]$$

As a result, the electromotive force $jp\Omega\underline{\Phi}_r$ behaves as a resistance with value $\frac{1-g}{g}R_r$. By adding the resistance R_r of the rotor winding, we then get global resistance $\frac{R_r}{g}$ corresponding to the sum of the converted power and rotor Joule losses. This general principle is valid for all the diagrams introduced earlier. In order to get the sinusoidal mode diagram, we just have to replace electromotive force by a resistance in the form $\frac{1-g}{g}R_2$.

Important note: *we can observe that all the parameters of the dynamic model are present in the sinusoidal mode model*. If we can estimate all these parameters by sinusoidal mode measurements, we then have a valid sinusoidal model as well as a valid dynamic model.

We showed that saturation can be taken into consideration by using magnetizing inductance L_m (or L_s in the case of total rotor leakage models) as a function of ξ_m equal to i_m or to ϕ_m; these variables represent modules of complex numbers defined by the transformation presented in section 1.2.1. In the case of SM, the rms value Ξ_m of $\xi_{ma}(t)$, relative to one phase, and module $\xi_m(t)$ of vector $\underline{\xi}_m(t)$ are in a ratio of $\sqrt{3}$ (see equation [1.27]). We can then adapt the characteristic of saturation [1.25] to obtain saturation characteristic $\tilde{L}_m(\Xi_m)$ depending on the rms value of the saturation variable:

$$\tilde{L}_m(\Xi_m) = L_m(\sqrt{3}\,\Xi_m) \qquad [1.29]$$

In the case where we choose flux as a saturation variable, it might be practical to consider induced electromotive force $E_m = \omega\phi_m$, as it can easily be determined from stator voltage[2]. Identification results of the saturation characteristics will be provided later in the chapter (see section 1.4.1).

Working with a set angular frequency $\omega = 2\,\pi\,f$ ($f = 50$ Hz in Europe; $f = 60$ Hz in North America), we will use the following notations in the rest of the chapter to simplify:

$$X_m = L_m\,\omega,\;\; X_r = l_r\,\omega \;\text{ and }\; X_s = l_s\,\omega. \qquad [1.30]$$

1.2.6. *Summary of the different models*

The different models that we have obtained can all be put in a single form corresponding to the phase equivalent diagram represented in Figure 1.3. In the case of the total stator model (see Figure 1.2), we will consider that

$$X_m = L_{m\,r}\,\omega,\; X_s = N_s\,\omega \text{ and } X_r = 0,\; R_2 = R_{2r}. \qquad [1.31]$$

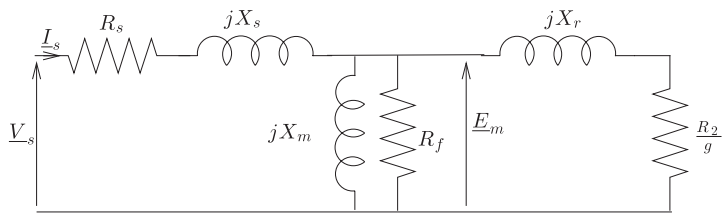

Figure 1.3. *Sinusoidal mode model*

In the case of the total rotor leakage model (see Figure 1.1), we will consider that

$$X_m = L_s\,\omega,\; X_s = 0,\; X_r = N_r\,\omega \text{ and } R_2 = R_{2s}. \qquad [1.32]$$

The equivalent phase model impedance is written as

$$\underline{Z} = R_s + j\,X_s + \frac{1}{\frac{1}{R_f} + \frac{1}{j\,X_m} + \frac{1}{j\,X_r + \frac{R_2}{g}}} \qquad [1.33]$$

---

2 The mesh law applied to the stator mesh of the diagram in Figure 1.2 gives $\underline{V}_s = (R_s + j\,N_s\,\omega)\,\underline{I}_s + \underline{E}_m$.

where X_m can be a function of the level of saturation. In the case of parametric saturation identification, we will from now on consider the model:

$$L_m = \frac{L_{m0}}{1 + A\,{\phi_m}^N} \qquad [1.34]$$

resulting in sinusoidal mode

$$X_m = \frac{X_{m0}}{1 + \alpha\,{E_m}^N} \qquad [1.35]$$

with

$$X_{m0} = L_{m0}\,\omega \text{ and } \alpha = A\left(\frac{\sqrt{3}}{\omega}\right)^N. \qquad [1.36]$$

There are 12 different models considered. One choice in three for leakage position (rotor, stator, or distributed), one in two for saturation (with or without), and one in two for iron losses (with or without). These different models are explained in Table 1.2. The first letter indicates if the leaks are totaled at the stator (**S**), rotor (**R**) or if the leaks are distributed between the stator and the rotor (**D** for Sales). The models that consider the saturation have an **s** as a second letter; and the models taking into account iron losses have letter **f**. Each model is in the general form of the diagram in Figure 1.3 as long as certain parameters are set at a zero value (X_s, X_r, or A) or infinite (R_f). The asterisks represent the parameters to estimate; four to six according to the models. Model **D** cannot be identified. The other models can theoretically be identified but, we will see later, separate leak models are difficult to identify in practice.

Parameter	**R**	**S**	**D**	**Rf**	**Sf**	**Df**	**Rs**	**Ss**	**Ds**	**Rsf**	**Ssf**	**Dsf**
R_s (Ω)	*	*	*	*	*	*	*	*	*	*	*	*
R_2 (Ω)	*	*	*	*	*	*	*	*	*	*	*	*
R_f (Ω)	∞	∞	∞	*	*	*	∞	∞	∞	*	*	*
N_1 (mH)	*	0	*	0	*	*	*	*	0	0	*	*
N_2 (mH)	0	*	*	*	0	*	0	0	*	*	0	*
$L_{m\,0}$ (mH)	*	*	*	*	*	*	*	*	*	*	*	*
A (Wb^{-4})	0	0	0	0	*	0	*	*	*	*	*	*

Table 1.2. *Different models considered*

1.2.7. *Measurements*

The methods that we will present from now on help us to determine the numeric values of the parameters from sinusoidal measurements. Two types of measurements are necessary: electrical measurements for the stator (voltage, current, power, etc.) and a mechanical measurement: the rotor's rotation speed.

For electrical measurements, usually we would consider the measurements of the rms value V_s of a phase voltage, I_s the rms value of its current and power P. In purely sinusoidal mode (absence of harmonics), we have $P = 3\,V_s\,I_s\,\cos(\phi)$, where ϕ is the voltage/current phase difference. We can then determine the equivalent complex impedance of a phase $\underline{Z} = Z\exp(j\,\phi)$ with $\phi = \arccos(P/(3\,V_s\,I_s))$ and $Z = V_s/I_s$. If harmonics are present, it is then preferable to work on the fundamentals of the voltage and current and to only consider the energy transported by the fundamental, enabled by certain measurement devices. This technique is used in section 1.5. It is possible to replace the power measurement by a direct phase difference ϕ measurement between voltage and current. This is the method that will be used in section 1.4.

Speed measurement Ω must be precise. In fact, it is used to determine slip form relation $g = 1 - \frac{p\,\Omega}{\omega}$, with $p\Omega$ similar to ω. In this way, a relatively small speed error can generate a relatively important error on the slip.

The test bench for the estimation of parameters must enable the variation of the point of operation. In order to do this, we need a variable mechanical load for imposing a variable torque. If this load is passive (powder brake, direct current generator discharging in a rheostat), only the stable operation zones will be used (for slips of some percentage). A controlled speed load makes it possible to carry out measurements for all the values of speed (and thus slip)[3]. It is also interesting to have a reversible load, to reverse the direction of transfer of energy and to make the induction machine work as a generator, corresponding to faster speeds than the speed of synchronism.

If we want to identify the saturation characteristic, it is necessary to change the flux and consequently the voltage. We usually use a variable autotransformer in this case.

3 We will be careful when implementing such a system in an operation zone corresponding to instability of the induction machine because the whole system may be unstable.

1.2.8. *Use of the nameplates*

The nameplates of induction motors vary from one manufacturer to another. Nevertheless, we can consider that they will at least provide the following information relative to the nominal working point: nominal slip g_N, rms value U_{sN} of the voltage between two phases, rms value I_{sN} of the line current, power factor F_p, and output power P_u. It is not possible to determine the series of parameters of induction machine models only from the nameplate information. We will then introduce a "well designed" hypothesis; i.e., we will presume that the nominal machine operation corresponds to the optimal power factor. In addition, we will ignore stator resistance.

Ignoring mechanical losses helps to identify mechanical power to output power ($P_m = P_u$). Knowing that the power transmitted to rotor P_2 is distributed in mechanical power and in rotor Joule losses according to relations $P_m = (1-g)\,P_2$ and $P_{jr} = g\,P_2$, we can determine P_2 and P_{jr}. The electrical power absorbed is $P_e = \sqrt{3}\,U_{sN}\,I_{sN}\,F_p$. Since the stator Joule losses are ignored, a power balance makes it possible to estimate iron losses: $P_f = P_e - P_2$. Knowing that iron losses and written $P_f = 3\frac{{V_{sN}}^2}{R_f}$, we can estimate $R_f = \frac{3\,{V_{sN}}^2}{P_f}$.

The admittance of a phase at nominal point is $\underline{Y}_N = Y_N \exp(-j\,\phi_N)$ with $Y_N = \frac{V_{sN}}{I_{sN}}$ and $\phi_N = \arccos(F_p)$. It is known that the location of admittance when the slip varies is a circle of diameter $1/X_r$ and which center is a point with an affix with, as real part, $\frac{1}{R_f}$. By relying on Figure 1.4, we extract from the right triangle OAD relation $\sin(\phi_N) = \frac{Y_N}{\mathrm{OD}}$. We can also obtain relation $\sin(\phi_N) = \frac{1}{R_f\,\mathrm{CD}}$. The radius is then written $r = \mathrm{AC} = \mathrm{AD} - \mathrm{CD} = \frac{Y_n}{\sin(\phi_N)} - \frac{1}{R_f\ \sin(\phi_N)}$, which makes it possible to obtain $X_r = \frac{1}{2\,r}$.

Rotor Joule losses, which were previously evaluated, are written $P_{jr} = 3\,R_2\,{I_r}^2$, where I_r is the current in the rotor branch such that ${I_r}^2 = \frac{{V_{sN}}^2}{{R_2/g_N}^2+{X_r}^2}$. This relation helps to determine R_2 by solving the equation of the second order:

$$ {R_2}^2 - b\,R_2 + (g_N\,X_r)^2 = 0 \qquad [1.37] $$

with $b = \frac{3\,{V_{sN}}^2\,{g_N}^2}{P_{jr}}$. This equation has two real positive solutions. For each root R_{21} and R_{22}, we can then determine the magnetizing reactance by replacing in the general admittance expression, resulting in

$$ X_{mk} = \frac{j}{\underline{Y}_N - \frac{1}{R_f} - \frac{g_N}{R_{2k}+j\,g_N\,X_r}} \qquad [1.38] $$

We will select the most plausible couple (R_{2k}, X_{mk}).

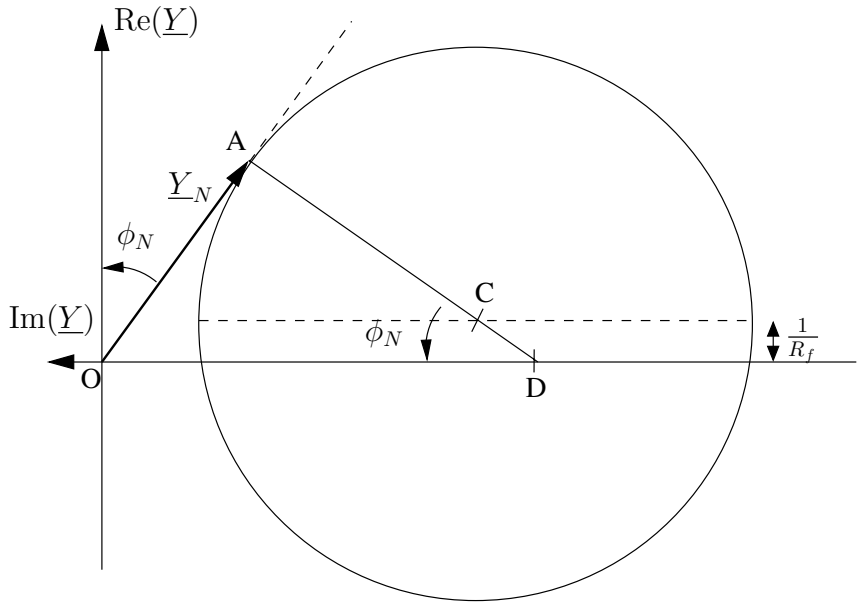

Figure 1.4. *Admittance diagram*

In the case of the MAS3 machine, the characteristics of which are given in Appendix 1.7.2, we obtain: $R_f = 644\,\Omega$ and $X_r = 20\,\Omega$. Only the greatest of the roots of [1.37] gives a positive X_m value; we then have $R_2 = 3,8\,\Omega$ and $X_m = 284\,\Omega$.

1.3. Traditional methods from a limited number of measurements

1.3.1. *Measurement of stator resistance*

Resistance R_s of a stator winding is the only parameter that can be measured independently from the other parameters. We just have to power a phase of the motor with direct current, to sample the average values of voltage and current and to determine R_s as the voltage over current ratio.

Since the resistance values are sensitive to variations in temperature, it is recommended to bring the machine to its working temperature prior to making this measurement[4].

4 The time necessary to reach a stationary temperature increases with the size of the machine. It can take a few minutes for a few kilowatts machine and several hours for a very powerful machine.

1.3.2. *Total rotor leakage model*

Different procedures based on two tests help us to obtain the parameters of the total rotor leakage model[5].

1.3.2.1. *Usual method*

The most usual method to determine the parameter values contains two tests:

– no-load test (without load torque) under nominal voltage with stator voltage V_{s0}, stator current I_{s0}, power P_0 and speed Ω_0[6],

– locked rotor test ($g = 1$) with reduced voltage or a specific g_1 slip providing values V_{s1}, I_{s1} and P_1 of the same quantities[7].

In a first approach, we can consider that the no-load speed is equal to the speed of synchronism, corresponding to zero slip. The rotor branch of the model is then open, and it is possible to estimate the parameters of the magnetic circuit from no-load measurements. By deducting the stator Joule losses at the absorbed power ($P_{01} = P_0 - 3\,R_s\,{I_{s0}}^2$) and by calculating voltage E_m to L_m terminals:

$$E_m = \sqrt{{V_{s0}}^2 - R_s\,I_{s0}\,V_{s0}\,\cos(\phi_0) + (R_s\,I_{s0})^2} \qquad [1.39]$$

where ϕ_0 is the phase difference of voltage in relation to the no-load current. From an active and reactive energy balance, we then determine the following:

$$\begin{cases} R_f &= \dfrac{3\,{E_m}^2}{P_{10}} \\ X_m &= \dfrac{3\,{E_m}^2}{Q_0} \end{cases} \qquad [1.40]$$

---

5 That is particularly the case in the NFC 51-100 norm from the UTE based on the circle's diagram, i.e. the image of the current when the slip varies. The circle diagram is generally established from a simplified model, where Joule losses are either ignored or referred to rotor level. This procedure is described in [SÉG 94, PIC 65, FOU 73, DAL 85].

6 Opinions differ how to carry out no-load tests. Some authors recommend setting the machine to its synchronism speed, using a driving load which only provides sufficient energy to compensate losses. Nevertheless, since the rotor rotates at the speed of synchronism, the machine then behaves like a synchronous machine excited by its residual field, which may disrupt the measurements.

7 The locked rotor test has two disadvantages. First, it presumes that we can mechanically block the axis of the machine when it is generally protected for security purposes. In addition, with locked rotor, the rotor currents are at the stator's angular frequency ω, a very high angular frequency compared to their usual range. In this case, additional frequency effects can emerge, leading to significant variations in parameters, and notably leaks. This phenomenon is very significant for deep slot rotors where this effect is used to make start-up easier. If we want to identify a valid model for nominal operation, it is better to use a nominal slip measurement.

with $Q_0 = \sqrt{(3\,V_{s0}\,I_{s0})^2 - {P_0}^2}$.

1.3.2.1.1. Simplified calculation

For the locked rotor test ($g = 1$) under reduced voltage, it is usual to ignore the current passing through the magnetizing inductance and iron losses. We can then write active and reactive powers:

$$\begin{cases} P_1 &= 3\,(R_s + R_2)\,{I_{s1}}^2 \\ Q_1 &= 3\,X_r\,{I_{s1}}^2 \end{cases} \qquad [1.41]$$

with $Q_1 = \sqrt{(3\,V_{s1}\,I_{s1})^2 - {P_1}^2}$. The unknown parameters are then determined by

$$\begin{cases} R_2 &= \dfrac{P_1}{3\,{I_{s1}}^2} - R_s \\ X_r &= \dfrac{Q_1}{3\,{I_{s1}}^2} \end{cases} \qquad [1.42]$$

1.3.2.1.2. Precise calculation

In order to obtain more precise results, it is preferable not to ignore the saturation of the magnetic circuit[8]. An ingenious way of obtaining results is to write calculations in complex form. $\underline{Z}_1$ is the equivalent impedance calculated from measurements by the method described in section 1.2.7. The model gives the following relation:

$$\underline{Z}_1 = R_s + \frac{1}{\frac{1}{jX_m} + \frac{1}{R_f} + \frac{1}{\frac{R_2}{g_1} + jX_r}} \qquad [1.43]$$

written as

$$\frac{R_2}{g_1} + j\,X_r = \frac{1}{\frac{1}{\underline{Z}_1 - R_s} - \frac{1}{j\,X_m} - \frac{1}{R_f}}. \qquad [1.44]$$

The real and imaginary parts are enough to isolate R_2 and X_r, respectively:

$$\begin{cases} R_2 &= g_1\,\mathrm{Re}\left(\dfrac{1}{\frac{1}{\underline{Z}_1 - R_s} - \frac{1}{j\,X_m} - \frac{1}{R_f}}\right) \\ X_r &= \mathrm{Im}\left(\dfrac{1}{\frac{1}{\underline{Z}_1 - R_s} - \frac{1}{j\,X_m} - \frac{1}{R_f}}\right) \end{cases} \qquad [1.45]$$

8 This is necessary in the case of a measurement under nominal voltage where the effect of the magnetic circuit cannot be ignored.

1.3.2.2. *Use of any two measurements*

The previous method can be generalized in order to take any two measurement points into consideration[9]. Note the different measurements with indices a and b corresponding to two measurement points. To simplify calculations, note $\underline{\tilde{Y}}_k$ as complex admittances of circuits once stator Joule losses compensated. If $\underline{Z}_k$, $k = a, b$ is the equivalent impedance determined from experimental measurements as explained in section 1.2.7, we can determine them with relation $\underline{\tilde{Y}}_k = 1/(\underline{Z}_k - R_s)$. Admittance expressions:

$$\begin{cases} \underline{\tilde{Y}}_a = \dfrac{1}{jX_m} + \dfrac{1}{R_f} + \dfrac{g_a}{R_2 + j\,X_r\,g_a} \\ \underline{\tilde{Y}}_b = \dfrac{1}{jX_m} + \dfrac{1}{R_f} + \dfrac{g_b}{R_2 + j\,X_r\,g_b} \end{cases} \quad [1.46]$$

Two of the unknown parameters are easily eliminated considering the difference term for term of both equations, which then results in:

$$R_2 - g_a\,g_b\,\frac{{X_r}^2}{R_2} + j\,(g_a + g_b)\,X_r = \frac{g_a - g_b}{\underline{\tilde{Y}}_a - \underline{\tilde{Y}}_b} \quad [1.47]$$

The imaginary part of this last equation determines the value of X_r:

$$X_r = \frac{g_a - g_b}{g_a + g_b}\,\mathrm{Im}\left(\frac{1}{\underline{\tilde{Y}}_a - \underline{\tilde{Y}}_b}\right) \quad [1.48]$$

We then have to determine R_2 as the only positive solution of the second-order equation obtained with the real section of relation [1.47]:

$${R_2}^2 - B\,R_2 - g_a\,g_b\,{X_r}^2 = 0 \quad [1.49]$$

with $B = (g_a - g_b)\,\mathrm{Re}\left(\frac{1}{\underline{\tilde{Y}}_a - \underline{\tilde{Y}}_b}\right)$, or

$$R_2 = \frac{1}{2}\left(B + \sqrt{B^2 + 4\,g_a\,g_b\,{X_r}^2}\right) \quad [1.50]$$

9 This makes it possible notably to consider the measurement of no-load speed if it is not exactly equal to the speed of synchronism.

The values of X_m and R_f are then simply obtained by using one of the two equations of [1.46], the first one, for example:

$$\begin{cases} R_f = \dfrac{1}{\mathrm{Re}\left(\underline{Y}_1 - \dfrac{g_a}{R_2 + j\,X_r\,g_a}\right)} \\ X_m = \dfrac{-1}{\mathrm{Im}\left(\underline{Y}_1 - \dfrac{g_a}{R_2 + j\,X_r\,g_a}\right)} \end{cases} \quad [1.51]$$

We can use this method by choosing a no-load measurement and a nominal load measurement. We can then consider, when appropriate, the value of the no-load speed if it is slightly different from the speed of synchronism.

1.3.3. *Total stator leakage models*

In the case of total stator leakage models, the estimation of parameters with the help of two measurements is clearly more difficult to achieve. In fact, it is a four nonlinear equation system (if we consider the real and imaginary parts of both equations) with four unknowns. In the present case, the no-load test makes it possible to eliminate a single parameter instead of two in the previous case, the same applies to the technique previously used consisting of calculating the difference between both equations.

If, however, we wish to obtain a total stator leakage model with a simple method, *the easiest way is to estimate the parameters of the total rotor leakage model and to find an equivalent total stator leakage model*. When we ignore iron losses, we know that they are perfectly equivalent as long as we use the equivalence formulas from section 1.2.2.3. For the value of iron loss resistance, we propose to settle for the previously estimated value. It is obviously an approximation; a small difference will then remain between the values of impedances given by the two measurements and those given by the model.

1.3.4. *Saturation characteristic*

Once the values for the parameters in non-saturated mode are estimated, i.e. at low flux, we can try to extend the field of validity of the model by identifying the saturation characteristic[10]. We consider the measurements for a point of saturation with a level of saturation ξ_m: V_s, and I_s rms value of the voltage and current relative to a phase, P the power absorbed and g the slip. It is then possible to determine the equivalent

10 The method presented for the case of saturation dependence according to magnetizing current, is taken from [KAS 00].

impedance per phase as explained in section 1.2.7; note $\underline{Z}_{\rm mes}$ to clarify that it comes from the measurements. This impedance is also written based on model [1.33] where the value of L_m must be recalculated to correspond to the measurement point as much as possible. We can then choose:

$$X_m(\xi_m) = \mathrm{Im}\left(\left(\frac{1}{\underline{Z}_{\rm mes} - R_s - jX_s} - \frac{1}{R_f} - \frac{1}{\frac{R_2}{g} + jX_r}\right)^{-1}\right) \qquad [1.52]$$

To determine characteristic $X_m(\xi_m)$, it is necessary to determine the level of saturation. In order to simplify the writing, we will use complex notations by using $\underline{V}_s = V_s$ as reference. We then have $\underline{I}_s = I_s \exp(-j\phi)$, where ϕ is determined from $P = 3\,V_s\,I_s\,\cos(\phi)$. We can then determine the voltage across the inductance terminals by Kirchhoff's link rule:

$$\underline{E}_m = \underline{V}_s - (R_s + jX_s)\,\underline{I}_s. \qquad [1.53]$$

The magnetizing current module is then written as $I_m = \frac{E_m}{X_m}$. After iteration of measurements, we have two saturation characteristics: $X_m(E_m)$ and $X_m(I_m)$ which can be chosen as needed.

When appropriate, we can then identify the characteristic as a parametric function of the saturation variable by estimating parameters by a least-square technique. This type of estimation method will be presented in detail and used in the following part of this chapter for the estimation of parameters from a high number of measurements.

1.3.5. *Experimental results*

1.3.5.1. *Total rotor leakage model*

The estimation method previously discussed was implemented in the MAS3 motor, and the characteristics are provided in Appendix 1.7.2. Two usual measurements were carried out: no-load test and nominal load test. Different variable voltage no-load tests were then carried out in order to identify the saturation characteristic.

We estimate the parameters of model **Rsf** with total rotor leaks and considering saturation and iron losses. We estimate stator resistance by a direct current test: $R_s = 3.45\ \Omega$. From the no-load test ($V_{s0} = 158$ V, $I_{s0} = 3.06$ A, $P_0 = 173$ W), we determine $R_f = 1.51\ k\Omega$ and $X_m = 201\ \Omega$. The nominal slip test ($V_{s1} = 128$ V, $I_{s1} = 3.84$ A, $P_1 = 1190$ W, $g_1 = 2.4\%$) results in $R_2 = 3.14\ \Omega$ and $X_r = 20.9\ \Omega$. We can observe slight gaps compared to the values obtained from the nameplates. We must conclude that the nameplate only lets us have the orders of magnitude of parameters.

1.3.5.2. *Total stator leakage model*

By using the transition equations of the stator leakage model to the rotor leakage model [1.19], we determine the following parameter values of the total rotor leakage model: $X_{ms} = L_s\omega = 182\ \Omega$, $R_{2r} = 2.6\ \Omega$ and $X_s = N_s\omega = 19\ \Omega$; parameters R_s and R_f are unchanged.

Because of iron losses, both models are not rigorously identical. In order to compare them, their complex admittances were calculated for different slip values between -10% and $+10\%$ and are represented in Figure 1.5. We note that both models provide similar admittance values.

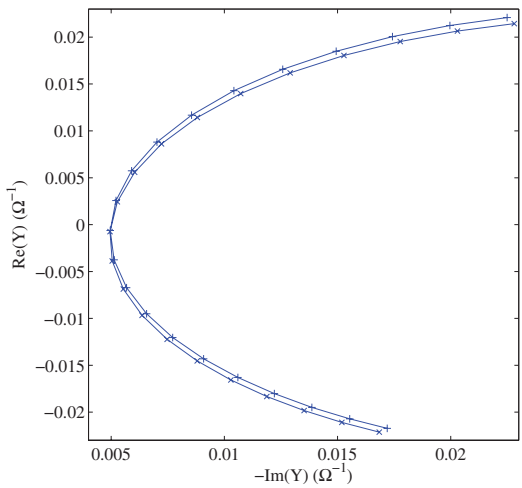

Figure 1.5. *Comparison between models* **Rf** *(×) and* **Sf** *(+)*

1.3.5.3. *Saturation*

We now focus on the effect of saturation on X_m value. For different measurement points, we calculate X_m with the help of relation [1.52]. The corresponding electromotive force E_m is determined with the help of relation [1.39], making it possible to draw X_m variations according to E_m. We can also calculate current $I_m = \frac{E_m}{X_m}$.

We propose to handle the identification of the saturation characteristic in the following form:

$$I_m = \alpha_1\, \phi_m + \alpha_2\, {\phi_m}^N \qquad [1.54]$$

where N is an integer to determine. The model depends linearly on parameters α_1 and α_2. We can then search for the values of parameters minimizing the gap quadratic criterion between the model and measurements:

$$J(\alpha_1, \alpha_2) = \sum_{k=1}^{m} (\alpha_1 \, \phi_{mk} + \alpha_2 \, {\phi_{mk}}^N - I_{mk})^2 \qquad [1.55]$$

where ϕ_{mk} and I_{mk}, $k = 1 \ldots m$, are the m measurements of ϕ_m and I_m. The parameters must verify the conditions of the first order $\frac{\partial J}{\partial \alpha_1} = 0$ and $\frac{\partial J}{\partial \alpha_2} = 0$, written in the following form:

$$\mathbf{A} \begin{bmatrix} \alpha_1 \\ \alpha_2 \end{bmatrix} = \mathbf{b} \qquad [1.56]$$

where

$$\mathbf{A} = \begin{bmatrix} \sum_{k=1}^{m} {\phi_{mk}}^2 & \sum_{k=1}^{m} {\phi_{mk}}^{N+1} \\ \sum_{k=1}^{m} {\phi_{mk}}^{N+1} & \sum_{k=1}^{m} {\phi_{mk}}^{2N} \end{bmatrix} \qquad [1.57]$$

and

$$\mathbf{b} = \begin{bmatrix} \sum_{k=1}^{m} \phi_{mk} \, I_{mk} \\ \sum_{k=1}^{m} {\phi_{mk}}^N \, I_{mk} \end{bmatrix}. \qquad [1.58]$$

We then calculate α_1 and α_2 by multiplying relation [1.56] to the left by the inverse of matrix $\mathbf{A}$. This technique was tested for different values of N. Value $N = 10$ showed the best results (i.e. the residual of the lowest criterion); giving $\alpha_1 = 1.44$ A/Wb and $\alpha_2 = 2.06$ A.Wb^{-10}. The points of measurement and the identified characteristic ($X_m = 1/(\alpha_1 + \alpha_2 \, (E_m/\omega)^{N-1})$) are represented in Figure 1.6. The characteristic identified corresponds accurately to the measurements.

1.4. Estimation by minimization of a criteria based on admittance

1.4.1. *Estimation of parameters by minimization of a criterion*

Let us consider a system in which a certain number of measurements M_k were done, grouped in vector M. Suppose that for each point of measurement, a relevant quantity can be calculated according to a function $f(M_k)$. Suppose that we

have a model of the system, parameterized by vector Θ, for estimating the relevant quantity by $\hat{f}(M_k, \Theta)$. For each point of measurement, we can then calculate the estimation error $\epsilon_k = \epsilon(\Theta, M_k) = f(M_k) - \hat{f}(\Theta, M_k)$ and build scalar function $J(\Theta, M) = \sum_k q_k ||\epsilon_k||^2$, which is a weighted sum of error squares (with q_k real positive). This positive scalar function is zero only if the model outputs correspond perfectly to the measurements. From an initial value, we will try to adjust Θ in order to minimize J by a procedure of optimization. If the model is identifiable and if the measurements are sufficiently rich, the criterion presents a global minimum; we will retain as a value of parameters the minimum argument: $\Theta^* = \arg\min_\Theta J(\Theta, M)$. In the case where the model is linear with respect to the parameters, this value can be determined analytically. We will discuss this topic in more detail in the last part of the chapter to propose a method of estimation of parameters simple to implement numerically. If that is not the case, the minimum must be approximated iteratively by a non-linear programming method such as Gauss–Newton or Levenberg–Marquard [FLE 87, GIL 81]. In practice, the residual of criterion $J(\Theta^*)$ is non-zero due to measurement errors and model errors.

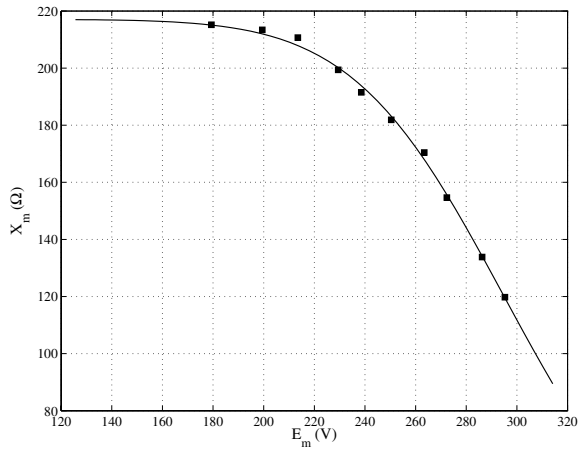

Figure 1.6. *Saturation characteristics*

1.4.2. *Choice of criterion*

Considering the circle diagram to characterize the operation of an induction machine is usual. Since this diagram represents complex admittance, it is legitimate to consider this quantity as relevant for identification ($f = \underline{Y}$). In this way, identifying the machine comes down to finding a model providing a circle diagram approximating measurements the best.

From the measurements grouped in a vector $M_k = [V_{sk}\ I_{sk}\ P_k\ \Omega_k]^T$, we determine admittance $\underline{Y}_k = f(M_k)$ as explained in section 1.2.7. In addition, the estimation of admittance is done with the help of the model selected $\underline{\hat{Y}}_k = \hat{f}(\Theta, M_k)$, where g_k is calculated from Ω_k. For a model that considers saturation, we must also calculate the saturation variable from M_k and Θ[11]. The criterion is then written as

$$J(\Theta, M) = \sum_{k=1}^{n} |\underline{Y}_k(M) - \underline{\hat{Y}}_k(\Theta, M)|^2 \qquad [1.59]$$

By noting $\underline{\epsilon}_k = \underline{Y}_k - \underline{\hat{Y}}_k$ and by grouping the different values in a vector: $\underline{\epsilon} = [\underline{\epsilon}_1 \dots \underline{\epsilon}_n]^T$, we can write

$$J(\Theta, M) = \underline{\epsilon}^{\mathrm{H}}(\Theta, M)\, \underline{\epsilon}(\Theta, M) \qquad [1.60]$$

where X^{H} represents the Hermitian of X, i.e. the conjugate of its transpose.

We consider, in this section, the parameter estimation of the different models presented in Table 1.2 with the saturation characteristic [1.35] and $N = 4$.

1.4.3. *Implementation*

Since the model is non-linear according to parameters, we should use a minimization algorithm to determine the numerical values of parameters. In order to improve the speed of convergence, it is preferable to use methods based on a limited development of the criterion.

The first derivative of the criterion with respect to the vector of parameters, called gradient, is a vector noted $\nabla(\Theta^*, M)$ with dimension n (number of parameters), where the ith component is written $(\nabla(\Theta^*, M))_i = \frac{\partial J(\Theta, M)}{\partial \Theta_i}$. The gradient can be written as

$$\nabla(\Theta, M) = 2\,\mathrm{Re}\left(\frac{\partial \underline{\epsilon}^{\mathrm{H}}(\Theta, M)}{\partial \Theta} \cdot \underline{\epsilon}(\Theta, M)\right) \qquad [1.61]$$

---

11 Determination of the saturation variable, ϕ_m or i_m, from measurements and parameters, is explained in section 1.3.5.3 (see equation [1.53]).

where the term at line k and column l of $\frac{\partial \underline{\epsilon}(\Theta,M)}{\partial \Theta}$ is $\frac{\partial \underline{\epsilon}_k(\Theta,M)}{\partial \Theta_l}$; in addition, $\frac{\partial \underline{\epsilon}^{\mathrm{H}}(\Theta,M)}{\partial \Theta} = \left(\frac{\partial \underline{\epsilon}(\Theta,M)}{\partial \Theta}\right)^{\mathrm{H}}$. The expression of the module sensitivities $\frac{\partial \epsilon_k}{\partial \Theta_l} = -\frac{\partial \hat{\underline{Y}}_k(\Theta,M_k)}{\partial \Theta_l}$ is given in Appendix 1.7.1.

The second derivative of the criterion in relation to the vector of parameters, called Hessian, is a $n \times n$ matrix where the term (i,j) is written $(H(\Theta,M))_{i,j} = \frac{\partial^2 J(\Theta,M)}{\partial \Theta_i \partial \Theta_j}$. We generally use the following approximate expression, valid for low values of $\underline{\epsilon}$:

$$\mathbf{H}(\Theta,M) \simeq 2\,\mathrm{Re}\left(\frac{\partial \underline{\epsilon}^{\mathrm{H}}(\Theta,M)}{\partial \Theta} \cdot \frac{\partial \underline{\epsilon}(\Theta,M)}{\partial \Theta}\right). \qquad [1.62]$$

Around an arbitrary value Θ^* of the vector of parameters, the second-order development is written as

$$\begin{aligned} J(\Theta,M) \;\simeq\; & J(\Theta^*,M) + \nabla^T(\Theta^*,M)\cdot(\Theta-\Theta^*) \\ & + \frac{1}{2}(\Theta-\Theta^*)^{\mathrm{H}} \cdot \mathbf{H}(\Theta^*,M)\cdot(\Theta-\Theta^*). \end{aligned} \qquad [1.63]$$

The gradient has a first-order development written as

$$\nabla(\Theta,M) \simeq \nabla(\Theta^*,M) + \mathbf{H}(\Theta^*,M)\cdot(\Theta-\Theta^*). \qquad [1.64]$$

1.4.4. *Analysis of estimation errors*

A method of estimation able to determine the values of parameters in ideal conditions is not enough. It must also be able to deliver a relatively precise estimation of the parameters despite errors affecting the system. There are two types of errors: *(i)* the measurement errors linked to inaccuracies in the measurement device and the chain of acquisition; *(ii)* those linked to model imperfections (ignored phenomena, idealization of reality). In order to validate or invalidate estimators, in this section, we conduct a complete theoretical accuracy analysis of estimators of the different models. This study is based on raw values of parameters obtained from prior investigation (these values are referred to as "*a priori* values" in the sequel; they can be derived from the name plate). In section 1.4.5, we will see that this study helps us to clarify experimental results.

1.4.4.1. *Method for error evaluation*

A first method for evaluating estimation errors consists of creating the estimation procedure from simulated measurements in which we have introduced one or more sources of error. For stochastic measurement errors, the resulting estimation errors are random variables, and we will focus on their stochastic properties (bias and standard deviation), which will be evaluated in a panel containing a large enough number of samples[12].

Another method consists of writing an approximate analytical development for the error in parameters according to measurement or model errors. The estimate $\hat{\Theta}$ of Θ verifies the first-order condition $\nabla(\hat{\Theta}, M) = 0$. From the development of gradient [1.64], we get the relation:

$$\nabla(\Theta^*, M) + \mathbf{H}(\Theta^*, M) \cdot (\hat{\Theta} - \Theta^*) = 0. \qquad [1.65]$$

Now consider that Θ^* is the "true" value of parameters, and that $\hat{\Theta} \neq \Theta^*$, because of measurement and model errors. The estimation error of parameters $\epsilon_\Theta = \hat{\Theta} - \Theta^*$ is then written as

$$\epsilon_\Theta \simeq -\mathbf{H}^{-1}(\Theta^*, M) \cdot \nabla(\Theta^*, M). \qquad [1.66]$$

It can be evaluated based on the *a priori* values of parameters Θ^*.

1.4.4.2. *Experiment design*

In order to best identify the behavior of the machine, we have considered a measurement set that is as large as possible. In practice, the slip is limited to a value $g_{\max}$ for stability purposes; we then limited ourselves to a range of $[-g_{\max}; g_{\max}]$. In order to identify saturation, it is interesting to vary the level of saturation (and thus voltage) in a wide range. By noting $V_{\max}$ as the maximum value that can be reached for voltage, we can choose to use as measurement range $[\frac{1}{2}V_{\max}; V_{\max}]$. It is not necessary to measure at very low voltage because the relative precision is then low and, in the absence of saturation, these measurements only bring redundant information. The experimental results used in this part were obtained on the MAS1 machine with characteristics available in Appendix 1.7.1. With a maximum slip of approximately 10% and maximum voltage of 120 V. We chose to carry out 66 different measurements for 11 E_m values and 6 slip values.

12 These are Monte-Carlo methods where we simulate, for example, 2,000 samples each containing 66 measurement points, for a representative panel.

In order to test the choice of measurement points on estimation precision, we also considered two other series of measurements containing the same number of measurements. In one, the measurements are done at positive slip, corresponding to motoring operation. In the other, the measurements are done at negative slip, i.e. in generating operation. Subsequently, we will see how to optimally design a set of measurement points.

1.4.4.3. *Effect of measurement errors*

We now present the evaluation of estimation errors, achieved with the help of analytical development presented in section 1.4.4.1 considering the measurement set presented in section 1.4.4.2. The series of results will be the subject of a discussion in section 1.4.4.5.

1.4.4.3.1. Offset and error of gain on sensors

We considered offsets on the different sensors corresponding to $\pm 1\%$ of the nominal value in voltage, current, phase difference, and speed (nominal values are given in Appendix 1.7.2), and we calculated the impact on the estimated value of the parameters of model $\mathbf{Rsf}$ (see Table 1.3). We provided the effect of each sensor offset and the worst-case conjugated effect of an offset in each sensor. We can observe that the most effective measurement is the phase measurement. The most sensitive parameters are R_f and R_s. The high level of these errors (117% and 43%, respectively) shows the necessity of an unbiased measurement of phase difference; it would also be useful to ensure that phase measurement has a lower offset by a tenth of what was considered in the evaluation, or less than 0.1% of 2π.

	Sensor				
Parameter	V_s	I_s	ϕ	Ω	sum
R_s	-0.4	0.8	42.3	-0.2	43.1
R_2	-1.4	0.8	-0.3	-0.0	-0.9
R_f	-0.3	0.6	-117	-3.1	-120
N_2	-1.5	3.2	-0.8	-0.0	0.8
$L_{m\,0}$	-2.1	2.4	-0.5	0.0	-0.1
A	0.4	4.2	-1.3	0.0	3.4

Table 1.3. *Errors of parameter estimations caused by sensor offsets (in percentage of nominal parameter value)*

We also evaluated the effect of a gain error of 1% in each sensor. The results are presented in Table 1.4 and show that the phase measurement is again the trickiest measurement that can lead to estimation errors in R_f and R_s.

	Sensor				
Parameter	V_s	I_s	ϕ	Ω	Sum
R_s	−1.0	1.0	10.1	−0.0	10.1
R_2	−1.0	1.0	0.3	−1.0	−0.7
R_f	−1.0	1.0	−26.3	−0.0	−26.3
N_2	−1.0	1.0	5.8	0.0	5.8
$L_{m\,0}$	−1.0	1.0	−0.6	−0.0	−0.6
A	4.0	−0.0	−1.2	−0.0	2.8

Table 1.4. *Errors of parameter estimations because of sensor gain errors (in percentage of the nominal value of parameters)*

1.4.4.3.2. Stochastic measurement noise

The parameter estimation of the different models was done from measurements containing a random additive error with standard deviation equal to 1% of nominal values (see Table 1.5). We start with model **R** with four parameters that will serve as reference. We get accurate precision in R_2 and $L_{m\,0}$ and a less accurate, but still satisfactory, precision in R_s and N_2. When we consider iron losses in model **Rf**, the precisions in the four starting parameters are almost maintained and R_f has an acceptable precision. At this stage, model **Rf** is considered as usable for identification.

In model **Df**, we try to separate leaks, theoretically possible if we account for iron losses. However, the precisions obtained in leakage inductances are catastrophic. We conclude that this model is inappropriate for identification.

Model **Rs** is different from reference model **R** because of the introduction of saturation. We can observe that the precision of the four physical parameters remains correct; model **Rs** is therefore usable. That is also the case with model **Rsf** accounting for iron losses and saturation. However, with models **Ds** and **Dsf** attempting to separate leaks with the presence of saturation, we cannot obtain satisfying leakage inductance values. They should therefore be rejected for identification. Generally speaking, separate leakage models cannot be practically identified.

Parameter	**R**	**Rf**	**Df**	**Rs**	**Rsf**	**Ds**	**Ds**
R_s	6.4	8.4	7.4	6.1	6.9	6.5	7.4
R_2	0.5	0.5	15.7	0.5	0.5	4.6	4.9
R_f	–	15.7	20.5	–	15.3	–	15.9
N_1	–	–	236	–	–	63.7	67.9
N_2	10.2	10.1	277	10.5	10.5	68.8	72.8
$L_{m\,0}$	1.7	1.7	8.1	3.0	3.0	2.9	2.9
A	–	–	–	15.2	15.0	29.6	30.1

Table 1.5. *Standard deviation of estimation errors caused by stochastic errors of measurements (in percentage of the nominal value of parameters) for a random additive error of 1% of nominal value*

1.4.4.4. *Effect of model error*

Ignoring a phenomenon can lead to significant estimation errors. Validating an estimation procedure in relation to this problem is a vital step. In the case of sinusoidal mode operation, the main model errors emerge when we ignore saturation and iron losses. The reader will find a more detailed analysis of model errors of the dynamic model in [LAR 00, LAR 08].

1.4.4.4.1. Iron losses

Models $\mathbf{Rs}$ and $\mathbf{Rsf}$ only differ in iron losses. By simulating measurements with $\mathbf{Rsf}$ and by estimating $\mathbf{Rs}$ parameters, we can evaluate estimation errors caused by iron losses, reported in Table 1.6. In order to evaluate the effect of the choice of measurement points, estimation errors were evaluated for the three distinct sets of measurements introduced in section 1.2.7: the complete case containing balanced measurements in motoring and generating mode (noted "Mixed" in the table), a set of measurements containing as many measurements but only in motoring mode and one set only containing generating mode measurements.

First, consider the estimation of parameters from the mixed measurement set. The most biased parameters are R_s (6.6%) and N_2 (3.3%). Errors in the other parameters are less than 1%. We can then consider that the errors are acceptable. When the estimation is done from measurements only corresponding to rotoring or generating mode operation, the biases are greater: more than 50% for R_s. In this way, estimation errors due to this model error are very sensitive to the choice of the set of measurement points.

Parameter	Mixed	Motor	Generator
R_s	-6.5	55.5	50.7
R_2	0.0	-7.9	7.6
N_2	3.4	23.4	-19.9
$L_{m\,0}$	0.1	0.5	-0.6
A	0.6	14.8	-15.7

Table 1.6. *Estimation errors due to iron losses (in percentage of parameter reference values)*

1.4.4.4.2. Saturation

Magnetic saturation is an undeniable phenomenon that necessarily appears in the nominal mode operation of an electric machine. However, for simplicity purposes, we often prefer to use models that ignore this phenomenon[13]. Parameter estimation

13 This is generally the case for models dedicated to control [FOR 00, FOR 04, GRE 01, MON 04].

of this kind of model from measurements corresponding to saturated mode operation yields estimation errors. As an example, in Table 1.7, values relative to the biases obtained by simulating measurements with $\mathbf{Rsf}$ and by estimating $\mathbf{Rf}$ parameters are presented.

For the three sets of measurements, parameter $L_{m\,0}$ is very sensitive to this model error. In fact, the estimated value of $L_{m\,0}$ is an average of the values taken by L_m during the different saturation measurements. The other biases are very low. The results are not sensitive to the choice of the set of measurements, as Table 1.7 shows.

Parameter	Mixed	Motor	Generator
R_s	-0.0	-0.0	-0.0
R_2	0.0	0.0	0.0
R_f	-1.8	-1.8	-1.8
N_2	0.0	0.0	-0.0
$L_{m\,0}$	-19.5	-19.5	-19.5

Table 1.7. *Estimation errors due to saturation (in percentage of parameter reference values)*

1.4.4.5. *Discussion*

For the sets of measurements considered, the study of estimation errors caused by measurement noise showed that models considering both stator and rotor leaks ($\mathbf{Df}$, $\mathbf{Ds}$, and $\mathbf{Dsf}$) are practically unidentifiable. We then cannot use them to simultaneously estimate all the parameters. In terms of saturation, it appears that we could use a model that does not consider this phenomenon. The study showed that iron losses, when they are ignored, can have a significant influence on the quality of parameter estimation. In addition, the results are very sensitive to the choice of measurements points. It is therefore desirable to account for iron losses in the identification model. If these losses are ignored, an in-depth study, in the spirit of the study presented here, is necessary to evaluate estimation errors and validate, or invalidate, all the chosen measurement points.

The only models guaranteeing a correct estimation of parameters are $\mathbf{Rf}$ and $\mathbf{Rsf}$, as well as their total stator leakage equivalents. Resistance R_s is not identified with good precision by this method, but that is of lesser importance because it may be estimated independently from the other parameters by a direct current measurement. In addition, we can also improve the precision of parameter estimation by choosing a better set of measurement points.

In conclusion, we will retain that saturation and iron losses can be estimated simultaneously with the other parameters and that we should not try to estimate the stator and rotor leaks separately.

1.4.5. *Experimental results*

In order to illustrate in a concrete case the identification protocol proposed in this section, measurements were taken from machine MAS1 (see Appendix 1.7.2) for 71 measurement points corresponding to a slip that varies between $-g_{\max}$ and $g_{\max} = 6\%$ and for E_m varying between $\frac{1}{2}V_{\max}$ and $V_{\max} = 130$ V. The numeric values of parameters estimated for the different models are given in Table 1.4.5. The parameters of the sinusoidal mode model are given earlier, followed by the residual of criterion J; and finally parameters of the dynamic model[14] or, more precisely, their value in the absence of saturation (calculated for $L_m = L_{m0}$). A lower value of the criterion indicates better identification. From this point of view, with these results, the rotor leakage models have a slight advantage over the stator leakage models. Remember that this difference can only appear in the presence of iron losses or saturation because, without these phenomena, both models are rigorously equivalent. The separation of leaks introduced in models **DS** and **DSF** turns out to be hazardous and leads to a negative value of N_1 for model **DSF**. These models should therefore be rejected, as predicted in the precision analysis phase. When appropriate, if a distribution of leaks is necessary, it must be first imposed in a heuristic way (e.g. by imposing $N_1 = N_2$) and cannot be identified experimentally by the protocol considered here.

Parameter	**Ss**	**Rs**	**Ssf**	**Rsf**	**Ds**	**Dsf**
$R_s\,(\Omega)$	1.3	1.29	1.33	1.28	1.29	1.28
$R_2\,(\Omega)$	0.65	0.76	0.64	0.75	0.75	0.76
$R_f\,(\Omega)$	∞	∞	424	491	∞	494
N_1 (mH)	5.8	0	5.7	0	0.2	-0.3
N_2 (mH)	0	6.8	0	6.7	6.6	7.0
$L_{m\,0}$ (mH)	92.6	97.2	92.3	97.1	97.1	97.2
$\alpha(10^{-9})$	5.09	2.94	4.99	2.94	3.00	2.85
$J(10^{-3})$	10.7	9.3	6.9	5.2	9.3	5.2
$R_r\,(\Omega)$	0.65	0.71	0.64	0.7	0.70	0.71
L_s (mH)	98.4	97.2	98.0	97.1	97.3	96.9
$L_r = M$ (mH)	92.6	90.8	92.3	90.8	90.9	90.7
σ (%)	5.9	6.5	5.8	6.5	6.6	6.4

Table 1.8. *Experimental estimation results*

1.4.6. *Optimal experiment design*

1.4.6.1. *Principle*

Optimal experiment design consists of determining the m measurement points that minimize estimation errors (bias and variance) for a given model structure. In the

14 See section 1.2.1.

current case where the study is based on *a priori* values of parameters, the optimality has only a local validity. In order to obtain more information on the numerous methods developed in this field, the reader should consult [WAL 97] or [WAL 90]. The optimal set of measurements is the solution of a minimization problem under constraints that is generally non-convex and presents local minima, making the direct use of usual optimization algorithms impossible. To remedy these problems, we used a genetic algorithm [BUC 92, MAN 97] and its result was used as an initial condition for a more conventional algorithm [FOR 76, COL 99] to refine precision. The results presented below use model **Rs** without iron losses but with saturation. They are based on an approximate expression of estimation errors using relation [1.66]. For detail on these calculations, the reader should refer to references [LAR 02] and [LAR 05].

1.4.6.2. *Minimization of the effect of measurement noises*

First, we try to minimize the effect of measurement noise analyzed in section 1.4.4.3.2. The criterion involved is the sum of variances of reduced estimation errors for different parameters. In this way, optimal set of measurements M^* is defined by the minimum argument of a variance function:

$$J(M) = \sum_{i=1}^{5} \left(\frac{\sigma_{\Theta_i}}{\Theta_{i0}} \right)^2 \qquad [1.67]$$

where σ_{Θ_i} is the standard deviation of the estimation error of parameter Θ_i with nominal value Θ_{i0}. To illustrate the methodology, a set of 12 measurement couples completely free in pad $[-g_{\max};\, g_{\max}]\times[\frac{1}{2}V_{\max};\, V_{\max}]$ was considered. Optimal torques $(g;\, E_m)$ obtained are grouped around four distinct values: $(g_{\min};\, V_{\max})$, $(g_{\max};\, V_{\max})$, $(g_1;\, V_{\min})$, and $(g_1;\, V_{\max})$ where $g_1 \simeq 0$. These different values are repeated, 3, 4, 3 and 2 times, respectively. It is an expected result indicating that an optimal experience is made up of a limited number of measurement points repeated several times; these points are generally located at the border of the reachable field. Note that three distinct measurement points are enough to determine the five parameters of model **Rs**.

1.4.6.3. *Minimization of the combined effect of measurement noise and iron losses*

We saw that if iron losses are not considered, the biases are significant and depend on the set of measurements. In order to synthesize a set of measurements guaranteeing a low bias, in addition of low variance, we have used a mixed criterion involving the variances of estimation errors caused by measurement noise and biases due to iron losses:

$$J(M) = \sum_{i=1}^{5} \left(\left(\frac{\sigma_{\Theta_i}}{\Theta_{i0}} \right)^2 + \lambda \left(\frac{b_{\Theta_i}}{\Theta_{i0}} \right)^2 \right) \qquad [1.68]$$

where b_{Θ_i} is the estimation error of parameter Θ_i due to iron losses, and λ is a factor making it possible to adjust the respective parts of both errors.

We chose $\lambda = 1,000$ making it possible to cancel almost all errors due to iron losses. The measurements obtained again contain four measurement points repeated two to four times and slightly modified compared to the previous case. The evaluation of this optimal protocol is reported in Table 1.9. We can compare with the results presented in Tables 1.3–1.6. We can observe a slight global improvement of results in terms of measurement errors and a drastic decrease of errors due to iron losses. We should moderate this last point, however. In fact, this strong improvement was obtained for given values of the parameters and may not be robust to variations of these parameters[15].

Parameter	Offset	Gain error	Stoch. Noise (sd)	Iron losses
R_s	31.6	7.4	7.2	−0.07
R_2	−1.4	−0.9	0.6	−0.01
R_f	−99.9	−21.8	12.6	–
N_2	2.4	5.5	10.2	−0.01
$L_{m\,0}$	1.5	0.1	0.9	−0.00
A	9.7	4.6	4.0	−0.00

Table 1.9. *Estimation errors with the optimal protocol (in percentage of nominal parameter values)*

1.4.7. *Conclusion on the method*

The estimation error evaluation of physical parameters of the induction motor made it possible to conclude on practical identifiability of the different models in sinusoidal mode. These results were used to determine sets of measurements minimizing the estimation errors while respecting physical constraints.

The choice of a model is generally given to the specialist in the field involved. On the contrary, the method that we propose allows to make an objective choice. Let us complement with some remarks. First, we must avoid using the most complete model with separate leaks. Even though it corresponds to the physics of the process better, it generally leads to absurd parameter values because of measurement errors and lack of structural identifiability. In order to obtain a model that can be identified, the phenomena only leading to low estimation error must be ignored. As the model is simplified, the estimation of parameters, although slightly biased, is gradually less sensitive to measurement noise. A good model results from a compromise between

15 The limitation of these approaches is that they are based on *a priori* parameter values. After an estimation of these parameters, it can be necessary to restart the analysis based on the new values.

low sensitivity to measurement noise and low bias caused by model errors. The optimal experiment design makes it possible to obtain an experimental protocol reducing the bias because of model errors, as well as sensitivity to the measurement noise.

1.5. Linear estimation

In this section, we present a method for moving beyond the non-linear programming step, facilitating numeric implementation. In the case of the total stator leakage model that considers iron losses but not saturation, we will see that the parameters can be estimated with satisfying precision.

1.5.1. *Principle*

We now consider a given model in the form of an affine relation between its parameters, i.e. that for a measurement M_k, we have a relation in the form:

$$\sum_{l=1}^{n} a_l(M_k) \cdot \Theta_l = b(M_k) \qquad [1.69]$$

involving parameters Θ_l, in the number of n and measurements M_k, where a_l and b_l can be vectors, and where the problem can be real or complex. For all m measurement sets, we can concatenate information, resulting in system:

$$\mathbf{A}(M) \cdot \Theta = \mathbf{B}(M) \qquad [1.70]$$

where

$$\mathbf{A}(M) = \begin{bmatrix} a_1(M_1) & \dots & a_n(M_1) \\ \vdots & & \vdots \\ a_1(M_m) & \dots & a_n(M_m) \end{bmatrix} \qquad [1.71]$$

and

$$\mathbf{B}(M) = \begin{bmatrix} b(M_1) \\ \vdots \\ b(M_m) \end{bmatrix} \qquad [1.72]$$

As long as the system is identifiable and the measurements are sufficiently rich, matrix $\mathbf{A}(M)$ is of rank n and the system is overdetermined. We then try to solve it in terms

of least squares, i.e. we search for the vector of parameters $\hat{\Theta}$ minimizing $||\mathbf{A}\hat{\Theta}-\mathbf{B}||_2$, given by:

$$\hat{\Theta} = \mathbf{A}^{\dagger}\,\mathbf{B} \qquad [1.73]$$

where $\mathbf{A}^{\dagger} = (\mathbf{A}^{\mathrm{H}}\,\mathbf{A})^{-1}\,\mathbf{A}^{\mathrm{H}}$ is the pseudo-inverse of $\mathbf{A}$.

To apply this method, we must be able to rewrite the problem in such a way that it becomes linear according to a new set of parameters. We must also be able to find the original parameters from the new ones. This can easily be done with models depending on four parameters. We will now concentrate on the total rotor leakage model considering iron losses where the resistance value of the stator has already been identified[16]. The case of the total rotor leakage model without iron losses is not discussed in this chapter but is available in the literature [LAR 04].

1.5.2. *Case of the five parameter model*

As an example, consider the total rotor leakage model considering iron losses ($\mathbf{Rf}$) without considering stator Joule losses. Its model, given by [1.33] by canceling R_s and X_s can be written as:

$$-\underline{Y}\,\Theta_1 + \Theta_2 + g\,\Theta_3 = j\,g\,\underline{Y} \qquad [1.74]$$

with $\Theta_1 = \frac{R_2}{X_r}$, $\Theta_2 = \frac{R_2}{X_r}(\frac{1}{R_f} + \frac{1}{jX_m})$ and $\Theta_3 = \frac{1}{X_m} + \frac{1}{X_r} + \frac{j}{R_f}$. It is a linear equation with complex factors involving complex parameters (Θ_1 alone is real). As long as we have enough measurement points (at least three), the method in the previous section can be applied.

This equation can also be transformed into a two linear equation system involving five real Θ_k^r parameters:

$$\begin{cases} -\mathrm{Re}(\underline{Y})\cdot\Theta_1^r + \Theta_2^r + g\,\Theta_4^r \;=\; -g\,\mathrm{Im}(\underline{Y}) \\ -\mathrm{Im}(\underline{Y})\cdot\Theta_1^r - \Theta_3^r + g\,\Theta_5^r \;=\; g\,\mathrm{Re}(\underline{Y}) \end{cases} \qquad [1.75]$$

with $\Theta_1^r = \frac{R_2}{X_r}$, $\Theta_2^r = \frac{R_2}{R_f X_r}$, $\Theta_3^r = \frac{R_2}{X_r X_m}$, $\Theta_4^r = \frac{1}{X_m} + \frac{1}{X_r}$ and $\Theta_5^r = \frac{1}{R_f}$. Once more, the method applies when we have three distinct measurement points. Note that these five real parameters can be obtained from the complex problem solutions: $\Theta_1^r = \mathrm{Re}(\Theta_1)$, $\Theta_2^r = \mathrm{Re}(\Theta_2)$, $\Theta_3^r = -\mathrm{Im}(\Theta_2)$, $\Theta_4^r = \mathrm{Re}(\Theta_3)$ and $\Theta_5^r = \mathrm{Im}(\Theta_3)$.

16 The resistance of a stator winding can be estimated by the direct current volt-ampere metric method.

Once the estimates for the five new parameters are found, the question then is how to obtain the four original parameters. Each of the new parameters constitutes an equation linking the original parameters: we now face an overdetermined problem. One method could be to try to minimize a distance criterion for the new parameters. But this criterion would be non-quadratic and minimization would require the implementation of a non-linear programming algorithm whereas we are actually trying to avoid using it in the current method.

A simple solution then is to delete only one of the five equations in order to determine an estimator of each parameter. Note that parameters Θ_1^r, Θ_2^r, and Θ_5^r are linked by the relation $\Theta_1^r \Theta_5^r = \Theta_2^r$. We can estimate original parameters without taking into account the value of one of those three parameter. Depending on the parameter removed, three estimators can be determined. However, the three resulting estimators are not always distinct and in the present case, we have two distinct estimators for each original parameter (see Table 1.10).

Parameter	Estimator #1	Estimator #2
R_2	$\dfrac{{\Theta_1^r}^2}{\Theta_1^r \Theta_4^r - \Theta_3^r}$	$\dfrac{{\Theta_2^r}^2}{\Theta_5^r(\Theta_2^r \Theta_4^r - \Theta_3^r \Theta_5^r)}$
R_f	$\dfrac{\Theta_1^r}{\Theta_2^r}$	Θ_5^r
X_m	$\dfrac{\Theta_1^r}{\Theta_3^r}$	$\dfrac{\Theta_2^r}{\Theta_3^r \Theta_5^r}$
X_r	$\dfrac{\Theta_1^r}{\Theta_1^r \Theta_4^r - \Theta_3^r}$	$\dfrac{\Theta_2^r}{\Theta_2^r \Theta_4^r - \Theta_3^r \Theta_5^r}$

Table 1.10. *The different estimators of physical parameters*

We end up with four estimators for each physical parameter. Two estimators (later called LC1 and LC2) are given by solving the complex system obtained from equation [1.74] and two others (LR1 and LR2) are given by solving the real system obtained from [1.75]; for each method LC and LR, two estimators are calculated as indicated in Table 1.10. These estimators do not have the same precision. We will see in the following sections that some estimators cannot be used because of their significant sensitivity to measurement or model errors. We will see that the estimators to use are estimators no 1 obtained with the real formulation [1.75].

1.5.3. *Study of precision*

In order to validate the estimation procedure and to select, among the different estimators, the least sensitive to measurement noises and model errors, we carried

out a series of tests. The different estimators are evaluated and compared to the method based on the minimization of a quadratic variance criterion presented in section 1.4 and called NL (non-linear). The evaluations were done on machine MAS2 (its characteristics are given in section 1.7).

1.5.3.1. *Measurement errors*

Among the measurement errors, we can distinguish the deterministic errors (offset, linearity error, gain error) from stochastic errors. We evaluated the effect of the offset error, gain error, and random additive noise.

1.5.3.1.1. Offset

The evaluation was achieved from simulated measurements integrating an offset error on sensors corresponding to a fraction of nominal values (± 1 V on voltage, ± 0.1 mA on current, ± 10 W on power, and ± 0.5 rad/s on speed). Among all the possible combinations, the worst deviation was reported in Table 1.11, in percentage of the nominal parameter value. The two estimators obtained by method LR and the two LC estimators are evaluated and compared with those of NL with or without identification of R_s, knowing that R_s may have been previously estimated. The NL method is used here as a reference; it provides a relatively good estimation of R_2 and X_m and a less precise estimation of X_r and R_f. Remember that the level of these errors is linked to the level of errors on sensors and can be decreased by increasing the sensor precision.

The linear formulation provides estimators with different levels of precision. For R_2 and X_m, we will only use the first estimator (LR1 or LC1), the second one is unusable because of its level of sensitivity to offset errors. For R_f, LC2 is also disqualified. We can observe that methods LR and LC enable us to obtain estimators with precision similar to, or even better than, the NL reference method.

	LR1	LR2	LC1	LC2	NL	
R_s	×	×	×	×	×	54.3
R_r	−0.56	203	−0.56	806	−2.17	−3.20
R_f	240	335	351	1230	239	211
X_m	17.0	227	17.2	967	15.6	15.1
X_r	−27.1	−24.5	−27.1	−25.4	−106	−111

Table 1.11. *Estimation errors because of sensor offsets (in percentage of nominal parameter values)*

1.5.3.1.2. Gain error

Errors of sensor gains were simulated: $\pm 2\%$ on voltage, current, and power and $\pm 1\%$ on speed. Maximum deviations in parameter values are given in Table 1.12 in percentage of the nominal value of parameters. The same estimators as in the previous case have to be rejected. Note that method NL sometimes leads to estimated R_f values

that tend toward the infinite. Once again, some estimators obtained with methods LR and LC have better results than those with NL.

	LR1	LR2	LC1	LC2	NL	
R_s	×	×	×	×	×	49.3
R_r	−2.62	−82.8	−2.62	112	11.4	−12.4
R_f	211	−61.9	335	858	∞	∞
X_m	4.19	−87.2	4.21	119	−6.20	−8.79
X_r	34.2	70.0	34.1	28.5	−210	−278

Table 1.12. *Estimation errors due to sensor gain errors (in percentage of the nominal parameter values)*

1.5.3.1.3. Stochastic errors

A random additive measurement noise was simulated for the different sensors with standard deviation equal to a fraction of nominal measurement values (1 V on voltage, 0.1 mA on current, 10 W on power, and 0.5 rad/s on speed). Each estimator of a parameter then becomes a random variable. By working on a sample containing a representative number of copies, we can estimate the statistical properties of estimators. By working with a set of samples repeating 2,000 times the estimation procedure (with a new draw of errors each time), we estimated the bias and standard deviation of each estimator and reported this data in Tables 1.13 and 1.14, as a percentage of nominal parameter values. We can observe that the biases are relatively low compared to standard deviations. X_m and R_2 estimations are relatively precise.

	LR1	LR2	LC1	LC2	NL	
R_s	×	×	×	×	×	0.50
R_r	0.01	−198	−0.01	30.8	0.00	−0.02
R_f	5.62	−152	6.40	15.75	2.06	2.05
X_m	0.15	−203	0.48	30.4	0.07	0.09
X_r	−0.39	−0.04	−1.85	−1.94	−0.96	−0.59

Table 1.13. *Errors of estimations due to stochastic measurement errors (in percentage of nominal parameter values)*

	LR1	LR2	LC1	LC2	Nonlinear	
R_s	×	×	×	×	×	9.64
R_r	0.80	10100	0.81	2610	0.53	0.56
R_f	27.3	7790	35.2	2880	16.8	17.3
X_m	4.81	10360	4.91	2720	3.05	2.92
X_r	19.9	18.3	20.0	17.2	13.0	14.3

Table 1.14. *Standard deviation of estimation errors due to stochastic measurement errors (in percentage of nominal parameter values)*

1.5.3.2. *Error on stator resistance*

Since the method does not allow us to include the R_s estimation, it must be estimated beforehand. The measurements can then be corrected by offsetting the effect of R_s. Nevertheless, this compensation, imperfect because it is linked to the estimated value of R_s, which is a value that is marred by some inaccuracy, can lead to estimation errors over all the other parameters. To evaluate this effect, we evaluated estimation errors by introducing an error of 10% on the estimated value of R_s (see Table 1.15). Estimators LR2 and LC2 are disqualified for R_2, R_f and X_m. The other LR and LC estimators offer a quality that is comparable with NL.

	LR1	LR2	LC1	LC2	NL
R_r	−0.24	210.3	−0.04	−108.7	−0.24
R_f	−0.16	223.5	51.31	−120.1	0.10
X_m	−0.20	223.4	−2.16	−113.0	−0.24
X_r	0.44	−3.59	0.64	−34.04	−0.11

Table 1.15. *Estimation errors (in percentage) due to an overestimation of R_s by 10 %*

1.5.3.3. *Discussion*

Among the different estimators available for a parameter, sensitivity to measurement and model errors greatly varies. For some, it is so high that they are automatically disqualified; that is the case with LR2 and LC2 for R_2, R_f and X_m. Both LR1 and LC1 formulations showed similar results with a slight advantage for LR1. Parameter X_r experiences worse precision than the others. The two estimators proposed by LR have similar performances for most evaluations. Nevertheless, the worst estimation error is due to gain errors for LR2 (70%). We therefore suggest choosing the estimator provided by LR1 for each parameter.

1.5.4. *Experimental results*

1.5.4.1. *Experimental setup*

The experimental setup (MAS2) on which the following results were obtained is different from the one used in the previous section. It is made up of a wound rotor induction motor by Leroy-Somer, with rated power of 1.5 kW and nominal voltage 230/400 V. The mechanical load is emulated by a direct current machine operating as a generator by connecting it to a rheostat or as a motor by powering it with a variable direct current voltage source. The rms value of voltage and current as well as power is measured by a Fluke 41B probe. The slip measurement is done very precisely by measuring angular frequency ω_r of the rotor current with the help of relation: $g = \frac{\omega_r}{\omega}$. In the more recent squirrel-cage motor, it can be done by a tacho-generator or through a measurement of position with the help of an incremental encoder. The value of

the resistance of stator winding is estimated in direct current at $R_s = 4.8\ \Omega$. The measurements are obtained in nominal voltage of 230 V per phase, for slips varying between -10% and $+10\%$.

1.5.4.2. *Non-linear method*

The method of minimization of a criterion on admittance, discussed earlier (section 1.4), and which serves as reference, was implemented in two cases: by using the R_s value previously estimated ($4.8\ \Omega$), or by estimating it simultaneously with the other parameters. The results are reported in the last two columns of Table 1.16. Even though the two R_s values obtained widely differ, this gap does not change the other parameters much.

1.5.4.3. *Linear method*

The different estimators obtained with the help of the method presented in this section were calculated for the two R_s values and reported in columns 2 to 9 in Table 1.16; index "1" corresponds to $R_s = 4.8\ \Omega$ and index "2" to $R_s = 8.95\ \Omega$. The results obtained corroborate the estimation error analyses. In fact, estimators LR2 and LC2 give absurd values for R_2, X_m, and X_r. The estimators chosen, i.e. those of LR1, provide results close to the ones from NL. In addition, the values given by these estimators have low sensitivity to the value of R_s. These estimators are the only ones that can be considered as relevant.

	$LR1_1$	$LR2_1$	$LR1_2$	$LR2_2$	$LC1_1$	$LC2_1$	$LC1_2$	$LC2_2$	NL_1	NL_2
$R_s(\Omega)$	4.8		8.95		4.8		8.95		4.8	8.95
$R_2(\Omega)$	6.39	-0.586	6.23	3.23	6.34	-0.728	6.28	4.19	6.47	6.39
$R_f(\Omega)$	1860	146	1710	644	-2400	520	-291	-56.3	1440	1750
$X_m(\Omega)$	109	8.56	111	41.8	109	-23.5	108	21.0	105	107
$X_r(\Omega)$	17.2	-20.2	18.4	25.3	17.1	9.07	18.5	63.7	13.8	15.5

Table 1.16. *Estimated values of parameters with different protocols*

1.5.4.4. *Comparison*

In order to graphically compare the results obtained from the selected models, three characteristics were drawn: the current diagram (Figure 1.7), the evolution of current according to slip (Figure 1.8), and the evolution of power according to slip (Figure 1.9). The values obtained from relevant models (LR1 and LC1) are compared to experimental results.

In the circle diagram, we can observe that in the model following the measurements the best is the one obtained by the NL method where the five parameters are estimated simultaneously. This is an expected result because this method actually attempts to fit the circle diagram. In fact, the five degrees of freedom represented by the five parameters to estimate allows a better approximation than with the four parameter model where R_s is fixed.

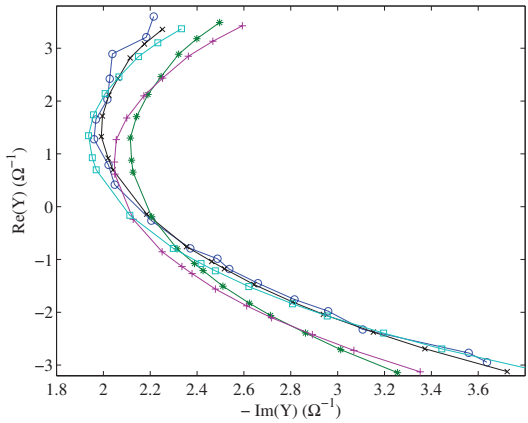

Figure 1.7. *Admittance diagram*
*(o: measurements, *: NL_1, ×: NL_2, +: $LR1_1$, □: $LR1_2$)*

This trend is also found on the current/slip characteristic (Figure 1.8), but the dispersion of results is relatively low in this case. In the power/slip characteristic (Figure 1.9), the four models follow all the measurements quite precisely.

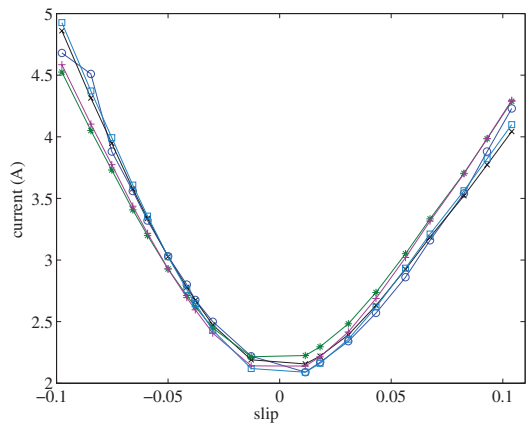

Figure 1.8. *Current/slip characteristic*
*(o: measurements, * : NL_1, × : NL_2, +: $LR1_1$, □: $LR1_2$)*

1.5.5. *Conclusion on the "linearizing" method*

The method we have detailed makes it possible to use a high number of measurements without having to use a non-linear programming algorithm as is the case

for the method in section 1.4. This method is not easy to implement for all models. Nevertheless, for models depending on four parameters such as the one we have treated, it can easily be implemented. This method goes through a parameterization change for writing the model in a linear way according to the new parameters. When it is time to come back to physical parameters, we should choose the correct estimator because some of them have high sensitivity to uncertainties affecting the system. In the present case, we should choose the first estimator presented in Table 1.10. In addition, we noted a slight superiority in the real formulation of the problem compared to the complex formulation. As long as the estimators are correctly chosen, the precisions obtained on the parameters are slightly better than those with NL method.

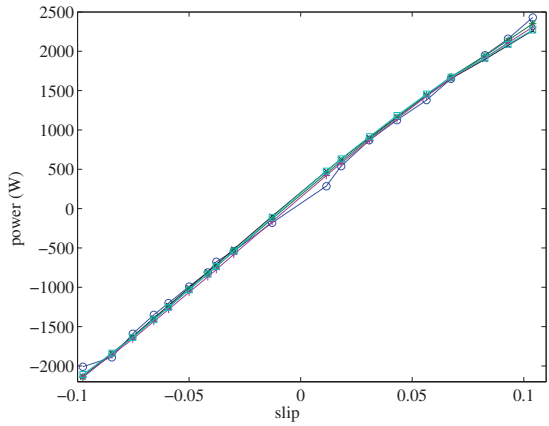

Figure 1.9. *Power/slip characteristic*
*(o: measurements, * : NL_1, ×: NL_2, +: $LR1_1$, □: $LR1_2$)*

1.6. Conclusion

In this chapter, we presented different methods to identify models of the induction motor in sinusoidal mode. We have seen that from these measurements, it is possible to obtain the dynamic model.

Generally speaking, an identification protocol is based on

– a model,

– an estimation method,

– measurement techniques, and

– points of measurement.

Its validation requires the validation of each of these points. The idea is to ensure that for the model and estimation method retained, because of the precision of sensors and points of measurement chosen, precision on the input–output behavior and parameters will be acceptable. A negative response requires that we question the different choices.

In the present case, we have specifically focused on the values of parameters. In this case, validation goes through an evaluation of estimation errors resulting from the different uncertainties affecting the system: measurement errors and model errors. This evaluation is based on models and *a priori* values of the parameters; it therefore only has a limited reach and does not necessarily apply to a machine with a very different range of power or technology. Each range of machines should be the subject of a study that is similar to what we have presented.

1.7. Appendix

1.7.1. *Expression of sensitivities*

The phase model of the induction motor in sinusoidal mode is written as impedance depending on the slip:

$$\underline{Z} = R_s + jX_s + \frac{1}{\underline{Y}_2} \qquad [1.76]$$

where

$$\underline{Y}_2 = \frac{1}{R_f} + \frac{1}{jX_m} + \frac{1}{jX_r + \frac{R_2}{g}}. \qquad [1.77]$$

The sensitivities of this model in relation to the different parameters make it possible to calculate the gradient and Hessian of a quadratic criterion (see section 1.4.3) and are written as:

$$\frac{\partial \underline{Z}}{\partial R_s} = 1 \qquad [1.78]$$

$$\frac{\partial \underline{Z}}{\partial X_s} = j \qquad [1.79]$$

$$\frac{\partial \underline{Z}}{\partial R_f} = \frac{1}{{R_f}^2 {\underline{Y}_2}^2} \qquad [1.80]$$

$$\frac{\partial \underline{Z}}{\partial X_m} = -\frac{j}{{X_m}^2 {\underline{Y}_2}^2} \quad [1.81]$$

$$\frac{\partial \underline{Z}}{\partial X_r} = \frac{j}{(jX_r + R_2/g)^2 {\underline{Y}_2}^2} \quad [1.82]$$

$$\frac{\partial \underline{Z}}{\partial R_2} = \frac{1}{g(jX_r + R_2/g)^2 {\underline{Y}_2}^2}. \quad [1.83]$$

In the case where the model is based on admittance $\underline{Y} = (\underline{Z})^{-1}$, we will calculate the sensitivities based on the formulas above with the help of:

$$\frac{\partial \underline{Y}}{\partial \Theta_k} = -\frac{\partial \underline{Z}}{\partial \Theta_k} \frac{1}{\underline{Z}^2} \quad [1.84]$$

where Θ_k represents one of the six parameters.

In the case where we consider a saturation characteristic in the form $X_m = X_{m\,0}/(1 + \alpha {E_m}^k)$, we obtain the sensitivities in relation to parameters $X_{m\,0}$ and α by composition:

$$\frac{\partial \underline{Y}}{\partial X_{m\,0}} = \frac{\partial \underline{Y}}{\partial X_m} \frac{1}{1 + \alpha {E_m}^k} \quad [1.85]$$

$$\frac{\partial \underline{Y}}{\partial \alpha} = \frac{\partial \underline{Y}}{\partial X_m} \frac{-{E_m}^k}{1 + \alpha {E_m}^k} \quad [1.86]$$

	MAS1	MAS2	MAS3
f (Hz)	50	50	50
V_n (V)	127/220	220/380	230/400
p	2	2	1
P_n (kW)	2.0	1.5	1.5
I_n (A)	7.2	7.5/4.4	5.0/2.9
Ω_n (rpm)	1500	1500	2885
$\cos(\phi)$			0.9
C_n (N.m)			5.0

Table 1.17. *Characteristics of the machines used*

1.7.2. *Characteristics of the machines used*

Three machines were used during this chapter to apply and evaluate the different approaches. The three motors were manufactured by the Leroy-Somer company. Information on their nameplates is presented in Table 1.17. MAS2 has a wound rotor; the others have squirrel-cage rotors.

1.8. Bibliography

[BUC 92] BUCKLESS B. P., PETRY E., *Genetic Algorithms*, IEEE Press, 1992.

[COL 99] COLEMAN T., BRANCH M. A., GRACE A., *Optimization Toolbox*, The MathWorks, 1999.

[DAL 85] DALMASSO J., *Cours d'électrotechnique*, vol. 1, Belin, Paris, 1985.

[FLE 87] FLETCHER R., *Practical Methods of Optimization*, Wiley, London, 1987.

[FOR 76] FORSYTHE G. E., MALCOLM M. A., MOLER C. B., *Computer Methods for Mathematical Computations*, Prentice-Hall, 1976.

[FOR 00] DE FORNEL B., PIETRZAK-DAVID M., ROBOAM X., "De la modélisation à la commande du moteur asynchrone", Chapter 5, in C. Canudas de Wit *et al.*, *Modélisation, contrôle vectoriel et DTC,* vol. 1, Hermes, 2000, p. 135-182.

[FOR 04] DE FORNEL B., "Modélisation dynamique des machines asynchrones", Chapter 5 in J.-P. Louis *et al.*, *Modèles pour la commande des actionneurs électriques*, Hermes, 2004, p. 215-287.

[FOU 73] FOUILLÉ A., *Electrotechnique à l'usage des ingénieurs*, vol. 2, Dunod, Paris, 1973.

[GIL 81] GILL P., MURRAY W., WRIGHT M., *Practical Optimization*, Academic Press, London, 1981.

[GRE 01] GRENIER D., LABRIQUE F., BUYSE H., MATAGNE E., *Electromécanique, convertisseurs d'énergie et actionneurs*, Dunod, Paris, 2001.

[KAS 00] KASMIEH T., LEFEVRE Y., HAPIOT J., "Modeling and experimental characterization of saturation effect of an induction machine", *European Physical Journal—Applied Physics*, vol. 10, 123-130, 2000.

[LAR 00] LAROCHE E., SEDDA E., DURIEU C., LOUIS J.-P., "Erreurs de modélisation d'une machine asynchrone – application au réglage d'un filtre de Kalman", *Revue Internationale Génie Electrique*, vol. 3, no. 1, 7-37, 2000.

[LAR 02] LAROCHE E., DURIEU C., LOUIS J.-P., "Erreurs d'estimation des paramètres de la machine asynchrone", *Journal Européen des Systèmes Automatisés*, vol. 36, no. 3, 481-496, 2002.

[LAR 04] LAROCHE E., BOUTAYEB M., "Identification of a class of nonlinear systems – analysis and robustness," *IFAC Symp. on Nonlinear Control Systems*, Stuttgart, Germany, Sept 2004.

[LAR 05] LAROCHE E., DURIEU C., LOUIS J.-P., "Parameter estimation accuracy analysis for an induction machine", *European Transactions on Electrical Power*, vol. 15, no. 4, 123-139, 2005.

[LAR 08] LAROCHE E., SEDDA E., DURIEU C., "Methodological insights for online estimation of induction motor parameters", *IEEE Transactions on Control Systems and Technology*, vol. 16, no. 5, 1021-1028, 2008.

[LAR 10] LAROCHE E., BOUTAYEB M., "Identification of the induction motor in sinusoidal mode", *IEEE Transactions on Energy Conversion*, in press.

[LEM 99] LEMAIRE-SEMAIL B., LOUIS J.-P., BOUILLAULT F., "Computation of induction machine inductances for extended analytical modeling accounting for saturation", *European Journal of Physics—Applied Physics*, vol. 5, 257-267, 1999.

[LOU 04] LOUIS J.-P., FELD G., MONMASSON E., "Modélisation des machines à courant alternatif par les phaseurs", Chapter 5 in J.-P. Louis *et al.*, *Modélisation des machines électriques en vue de leur commande*, Hermes, 2004, p. 247-291.

[MAN 97] MAN K. F., TANG K. S., KWONG S., HALANG W. A., *Genetic Algorithms for Control and Signal Processing*, Springer-Verlag, 1997.

[MON 04] MONMASSON E., LOUIS J.-P., "Modélisation statique des machines asynchrones en vue de leur commande scalaire", Chapter 6 in J.-P. Louis *et al.*, *Modèles pour la commande des actionneurs électriques*, Hermes, 2004, p. 289-333.

[PIC 65] PICHOIR J., *Cours d'Electrotrotechnique – machines électriques*, vol. 3, Masson, Paris, 1965.

[POL 67] POLOUJADOFF M., IVANES M., "Comparaison des schémas équivalents au moteur asynchrone polyphasé", *Revue Générale de l'Electricité*, vol. 76, no. 1, 1-6, 1967.

[SÉG 94] SÉGUIER G., NOTELET F., *Electrotechnique Industrielle*, Technique et Documentation, Lavoisier, Paris, 1994.

[WAL 90] WALTER E., PRONZATO L., "Qualitative and quantitative experiment design for phenomenological models–a survey", *Automatica*, vol. 26, no. 2, 195-213, 1990.

[WAL 97] WALTER E., PRONZATO L., *Identification of Parametric Models from Experimental Data*, Springer-Verlag, 1997.